6. Heineman-de Boer, J.A., Van Haelst, M.J., Cordia-de, H.M. and Beemer, F.A. (1999) Behavior problems and personality aspects of 40 children with velo-cardio-facial syndrome. *Genet. Couns.*, **10**, 89–93.
7. Kiley-Brabeck, K. and Sobin, C. (2006) Social skills and executive function deficits in children with the 22q11 deletion syndrome. *Appl. Neuropsychol.*, **13**, 258–268.
8. Niklasson, L., Rasmussen, P., Oskarsdottir, S. and Gillberg, C. (2002) Chromosome 22q11 deletion syndrome (CATCH 22): neuropsychiatric and neuropsychological aspects. *Dev. Med. Child Neurol.*, **44**, 44–50.
9. Woodin, M., Wang, P.P., Aleman, D., Donald-McGinn, D., Zackai, E. and Moss, E. (2001) Neuropsychological profile of children and adolescents with the 22q11.2 microdeletion. *Genet. Med.*, **3**, 34–39.
10. Shprintzen, R.J., Goldberg, R., Golding-Kushner, K.J. and Marion, R.W. (1992) Late-onset psychosis in the velo-cardio-facial syndrome. *Am. J. Med. Genet.*, **42**, 141–142.
11. Pulver, A.E., Nestadt, G., Goldberg, R., Shprintzen, R.J., Lamacz, M., Wolyniec, P.S., Morrow, B., Karayiorgou, M., Antonarakis, S.E. and Housman, D. (1994) Psychotic illness in patients diagnosed with velo-cardio-facial syndrome and their relatives. *J. Nerv. Ment. Dis.*, **182**, 476–478.
12. Murphy, K.C., Jones, L.A. and Owen, M.J. (1999) High rates of schizophrenia in adults with velo-cardio-facial syndrome. *Arch. Gen. Psychiatry*, **56**, 940–945.
13. Bassett, A.S., Hodgkinson, K., Chow, E.W., Correia, S., Scutt, L.E. and Weksberg, R. (1998) 22q11 deletion syndrome in adults with schizophrenia. *Am. J. Med. Genet.*, **81**, 328–337.
14. Gothelf, D., Presburger, G., Zohar, A.H., Burg, M., Nahmani, A., Frydman, M., Shohat, M., Inbar, D., Aviram-Goldring, A., Yeshaya, J. *et al.* (2004) Obsessive-compulsive disorder in patients with velocardiofacial (22q11 deletion) syndrome. *Am. J. Med. Genet. B Neuropsychiatr. Genet.*, **126**, 99–105.
15. Karayiorgou, M., Morris, M.A., Morrow, B., Shprintzen, R.J., Goldberg, R., Borrow, J., Gos, A., Nestadt, G., Wolyniec, P.S. and Lasseter, V.K. (1995) Schizophrenia susceptibility associated with interstitial deletions of chromosome 22q11. *Proc. Natl Acad. Sci. USA*, **92**, 7612–7616.
16. Bassett, A.S., Marshall, C.R., Lionel, A.C., Chow, E.W. and Scherer, S.W. (2008) Copy number variations and risk for schizophrenia in 22q11.2 deletion syndrome. *Hum. Mol. Genet.*, **17**, 4045–4053.
17. Debbane, M., Glaser, B., David, M.K., Feinstein, C. and Eliez, S. (2006) Psychotic symptoms in children and adolescents with 22q11.2 deletion syndrome: neuropsychological and behavioral implications. *Schizophr. Res.*, **84**, 187–193.
18. Fine, S.E., Weissman, A., Gerdes, M., Pinto-Martin, J., Zackai, E.H., Donald-McGinn, D.M. and Emanuel, B.S. (2005) Autism spectrum disorders and symptoms in children with molecularly confirmed 22q11.2 deletion syndrome. *J. Autism Dev. Disord.*, **35**, 461–470.
19. Vorstman, J.A., Morcus, M.E., Duijff, S.N., Klaassen, P.W., Heineman-de Boer, J.A., Beemer, F.A., Swaab, H., Kahn, R.S. and van Engeland, H. (2006) The 22q11.2 deletion in children: high rate of autistic disorders and early onset of psychotic symptoms. *J. Am. Acad. Child Adolesc. Psychiatry*, **45**, 1104–1113.
20. Antshel, K.M., Aneja, A., Strunge, L., Peebles, J., Fremont, W.P., Stallone, K., Abdulsabur, N., Higgins, A.M., Shprintzen, R.J. and Kates, W.R. (2007) Autistic spectrum disorders in velo-cardio facial syndrome (22q11.2 deletion). *J. Autism Dev. Disord.*, **37**, 1776–1786.
21. Kates, W.R., Antshel, K.M., Fremont, W.P., Shprintzen, R.J., Strunge, L.A., Burnette, C.P. and Higgins, A.M. (2007) Comparing phenotypes in patients with idiopathic autism to patients with velocardiofacial syndrome (22q11 DS) with and without autism. *Am. J. Med. Genet. A*, **143A**, 2642–2650.
22. Niklasson, L., Rasmussen, P., Oskarsdottir, S. and Gillberg, C. (2009) Autism, ADHD, mental retardation and behavior problems in 100 individuals with 22q11 deletion syndrome. *Res. Dev. Disabil.*, **30**, 763–773.
23. Chow, E.W., Watson, M., Young, D.A. and Bassett, A.S. (2006) Neurocognitive profile in 22q11 deletion syndrome and schizophrenia. *Schizophr. Res.*, **87**, 270–278.
24. Sebat, J., Lakshmi, B., Malhotra, D., Troge, J., Lese-Martin, C., Walsh, T., Yamrom, B., Yoon, S., Krasnitz, A., Kendall, J. *et al.* (2007) Strong association of de novo copy number mutations with autism. *Science*, **316**, 445–449.
25. Szatmari, P., Paterson, A.D., Zwaigenbaum, L., Roberts, W., Brian, J., Liu, X.Q., Vincent, J.B., Skaug, J.L., Thompson, A.P., Senman, L. *et al.* (2007) Mapping autism risk loci using genetic linkage and chromosomal rearrangements. *Nat. Genet.*, **39**, 319–328.
26. Marshall, C.R., Noor, A., Vincent, J.B., Lionel, A.C., Feuk, L., Skaug, J., Shago, M., Moessner, R., Pinto, D., Ren, Y. *et al.* (2008) Structural variation of chromosomes in autism spectrum disorder. *Am. J. Hum. Genet.*, **82**, 477–488.
27. Christian, S.L., Brune, C.W., Sudi, J., Kumar, R.A., Liu, S., Karamohamed, S., Badner, J.A., Matsui, S., Conroy, J., McQuaid, D. *et al.* (2008) Novel submicroscopic chromosomal abnormalities detected in autism spectrum disorder. *Biol. Psychiatry*, **63**, 1111–1117.
28. Cai, G., Edelmann, L., Goldsmith, J.E., Cohen, N., Nakamine, A., Reichert, J.G., Hoffman, E.J., Zurawiecki, D.M., Silverman, J.M., Hollander, E. *et al.* (2008) Multiplex ligation-dependent probe amplification for genetic screening in autism spectrum disorders: efficient identification of known microduplications and identification of a novel microduplication in ASMT. *BMC Med. Genomics*, **1**, 50.
29. Bucan, M., Abrahams, B.S., Wang, K., Glessner, J.T., Herman, E.I., Sonnenblick, L.I., Alvarez Retuerto, A.I., Imielinski, M., Hadley, D., Bradfield, J.P. *et al.* (2009) Genome-wide analyses of exonic copy number variants in a family-based study point to novel autism susceptibility genes. *PLoS Genet.*, **5**, e1000536.
30. Pinto, D., Pagnamenta, A.T., Klei, L., Anney, R., Merico, D., Regan, R., Conroy, J., Magalhaes, T.R., Correia, C., Abrahams, B.S. *et al.* (2010) Functional impact of global rare copy number variation in autism spectrum disorders. *Nature*, **466**, 368–372.
31. Itsara, A., Wu, H., Smith, J.D., Nickerson, D.A., Romieu, I., London, S.J. and Eichler, E.E. (2010) De novo rates and selection of large copy number variation. *Genome Res.*, **20**, 1469–1481.
32. Sanders, S.J., Ercan-Sencicek, A.G., Hus, V., Luo, R., Murtha, M.T., Moreno-De-Luca, D., Chu, S.H., Moreau, M.P., Gupta, A.R., Thomson, S.A. *et al.* (2011) Multiple recurrent de novo CNVs, including duplications of the 7q11.23 Williams syndrome region, are strongly associated with autism. *Neuron*, **70**, 863–885.
33. Guilmatre, A., Dubourg, C., Mosca, A.L., Legallic, S., Goldenberg, A., Drouin-Garraud, V., Layet, V., Rosier, A., Briault, S., Bonnet-Brilhault, F. *et al.* (2009) Recurrent rearrangements in synaptic and neurodevelopmental genes and shared biologic pathways in schizophrenia, autism, and mental retardation. *Arch. Gen. Psychiatry*, **66**, 947–956.
34. International Schizophrenia Consortium (2008) Rare chromosomal deletions and duplications increase risk of schizophrenia. *Nature*, **455**, 237–241.
35. Stefansson, H., Rujescu, D., Cichon, S., Pietilainen, O.P., Ingason, A., Steinberg, S., Fossdal, R., Sigurdsson, E., Sigmundsson, T., Buizer-Voskamp, J.E. *et al.* (2008) Large recurrent microdeletions associated with schizophrenia. *Nature*, **455**, 232–236.
36. Xu, B., Roos, J.L., Levy, S., van Rensburg, E.J., Gogos, J.A. and Karayiorgou, M. (2008) Strong association of de novo copy number mutations with sporadic schizophrenia. *Nat. Genet.*, **40**, 880–885.
37. Kirov, G., Grozeva, D., Norton, N., Ivanov, D., Mantripragada, K.K., Holmans, P., Craddock, N., Owen, M.J. and O'Donovan, M.C. (2009) Support for the involvement of large copy number variants in the pathogenesis of schizophrenia. *Hum. Mol. Genet.*, **18**, 1497–1503.
38. Need, A.C., Attix, D.K., McEvoy, J.M., Cirulli, E.T., Linney, K.L., Hunt, P., Ge, D., Heinzen, E.L., Maia, J.M., Shianna, K.V. *et al.* (2009) A genome-wide study of common SNPs and CNVs in cognitive performance in the CANTAB. *Hum. Mol. Genet.*, **18**, 4650–4661.
39. Bassett, A.S., Costain, G., Fung, W.L., Russell, K.J., Pierce, L., Kapadia, R., Carter, R.F., Chow, E.W. and Forsythe, P.J. (2010) Clinically detectable copy number variations in a Canadian catchment population of schizophrenia. *J. Psychiatr. Res.*, **45**, 1005–1009.
40. Levinson, D.F., Duan, J., Oh, S., Wang, K., Sanders, A.R., Shi, J., Zhang, N., Mowry, B.J., Olincy, A., Amin, F. *et al.* (2011) Copy number variants in schizophrenia: confirmation of five previous findings and new evidence for 3q29 microdeletions and VIPR2 duplications. *Am. J. Psychiatry*, **168**, 302–316.
41. Buizer-Voskamp, J.E., Muntjewerff, J.W., Strengman, E., Sabatti, C., Stefansson, H., Vorstman, J.A. and Ophoff, R.A. (2011) Genome-wide analysis shows increased frequency of copy number variation deletions in Dutch schizophrenia patients. *Biol. Psychiatry*, **70**, 655–662.
42. Grozeva, D., Conrad, D.F., Barnes, C.P., Hurles, M., Owen, M.J., O'Donovan, M.C., Craddock, N. and Kirov, G. (2012) Independent

estimation of the frequency of rare CNVs in the UK population confirms their role in schizophrenia. *Schizophr. Res.*, **135**, 1–7.
43. Hiroi, N., Zhu, H., Lee, M., Funke, B., Arai, M., Itokawa, M., Kucherlapati, R., Morrow, B., Sawamura, T. and Agatsuma, S. (2005) A 200-kb region of human chromosome 22q11.2 confers antipsychotic-responsive behavioral abnormalities in mice. *Proc. Natl Acad. Sci. USA*, **102**, 19132–19137.
44. Paylor, R., Glaser, B., Mupo, A., Ataliotis, P., Spencer, C., Sobotka, A., Sparks, C., Choi, C.H., Oghalai, J., Curran, S. *et al.* (2006) Tbx1 haploinsufficiency is linked to behavioral disorders in mice and humans: implications for 22q11 deletion syndrome. *Proc. Natl Acad. Sci. USA*, **103**, 7729–7734.
45. Suzuki, G., Harper, K.M., Hiramoto, T., Sawamura, T., Lee, M., Kang, G., Tanigaki, K., Buell, M., Geyer, M.A., Trimble, W.S. *et al.* (2009) Sept5 deficiency exerts pleiotropic influence on affective behaviors and cognitive functions in mice. *Hum. Mol. Genet.*, **18**, 1652–1660.
46. Bartsch, I., Sandrock, K., Lanza, F., Nurden, P., Hainmann, I., Pavlova, A., Greinacher, A., Tacke, U., Barth, M., Busse, A. *et al.* (2011) Deletion of human GP1BB and SEPT5 is associated with Bernard-Soulier syndrome, platelet secretion defect, polymicrogyria, and developmental delay. *Thromb. Haemost.*, **106**, 475–483.
47. Caltagarone, J., Rhodes, J., Honer, W.G. and Bowser, R. (1998) Localization of a novel septin protein, hCDCrel-1, in neurons of human brain. *Neuroreport*, **9**, 2907–2912.
48. Kinoshita, A., Noda, M. and Kinoshita, M. (2000) Differential localization of septins in the mouse brain. *J. Comp. Neurol.*, **428**, 223–239.
49. Michalon, A., Koshibu, K., Baumgartel, K., Spirig, D.H. and Mansuy, I.M. (2005) Inducible and neuron-specific gene expression in the adult mouse brain with the rtTA2S-M2 system. *Genesis*, **43**, 205–212.
50. Beaton, E.A. and Simon, T.J. (2011) How might stress contribute to increased risk for schizophrenia in children with chromosome 22q11.2 deletion syndrome? *J. Neurodev. Disord.*, **3**, 68–75.
51. Brain, P. (1975) What does individual housing mean to a mouse? *Life Sci.*, **16**, 187–200.
52. Voikar, V., Polus, A., Vasar, E. and Rauvala, H. (2005) Long-term individual housing in C57BL/6J and DBA/2 mice: assessment of behavioral consequences. *Genes Brain Behav.*, **4**, 240–252.
53. Terranova, M.L., Laviola, G. and Alleva, E. (1993) Ontogeny of amicable social behavior in the mouse: gender differences and ongoing isolation outcomes. *Dev. Psychobiol.*, **26**, 467–481.
54. Panksepp, J.B., Jochman, K.A., Kim, J.U., Koy, J.J., Wilson, E.D., Chen, Q., Wilson, C.R. and Lahvis, G.P. (2007) Affiliative behavior, ultrasonic communication and social reward are influenced by genetic variation in adolescent mice. *PLoS One*, **2**, e351.
55. Abramov, U., Raud, S., Koks, S., Innos, J., Kurrikoff, K., Matsui, T. and Vasar, E. (2004) Targeted mutation of CCK(2) receptor gene antagonises behavioural changes induced by social isolation in female, but not in male mice. *Behav. Brain Res.*, **155**, 1–11.
56. Hiramoto, T., Kang, G., Suzuki, G., Satoh, Y., Kucherlapati, R., Watanabe, Y. and Hiroi, N. (2011) Tbx1: identification of a 22q11.2 gene as a risk factor for autism spectrum disorder in a mouse model. *Hum. Mol. Genet.*, **20**, 4775–4785.
57. Flaherty, L. and Bolivar, V. (2007) Congenic and consomic strains.In Jones, B.C. and Mormede, P. (eds), *Neurobehavioral Genetics*. Taylor & Francis, New York, NY, pp. 115–127.
58. Rojas, D.C., Smith, J.A., Benkers, T.L., Camou, S.L., Reite, M.L. and Rogers, S.J. (2004) Hippocampus and amygdala volumes in parents of children with autistic disorder. *Am. J. Psychiatry*, **161**, 2038–2044.
59. Rojas, D.C., Peterson, E., Winterrowd, E., Reite, M.L., Rogers, S.J. and Tregellas, J.R. (2006) Regional gray matter volumetric changes in autism associated with social and repetitive behavior symptoms. *BMC Psychiatry*, **6**, 56.
60. Tan, G.M., Arnone, D., McIntosh, A.M. and Ebmeier, K.P. (2009) Meta-analysis of magnetic resonance imaging studies in chromosome 22q11.2 deletion syndrome (velocardiofacial syndrome). *Schizophr. Res.*, **115**, 173–181.
61. Pinkham, A.E., Hopfinger, J.B., Pelphrey, K.A., Piven, J. and Penn, D.L. (2008) Neural bases for impaired social cognition in schizophrenia and autism spectrum disorders. *Schizophr. Res.*, **99**, 164–175.
62. Andersson, F., Glaser, B., Spiridon, M., Debbane, M., Vuilleumier, P. and Eliez, S. (2008) Impaired activation of face processing networks revealed by functional magnetic resonance imaging in 22q11.2 deletion syndrome. *Biol. Psychiatry*, **63**, 49–57.
63. Winterer, G. and Weinberger, D.R. (2004) Genes, dopamine and cortical signal-to-noise ratio in schizophrenia. *Trends Neurosci.*, **27**, 683–690.
64. Zoghbi, H.Y. (2003) Postnatal neurodevelopmental disorders: meeting at the synapse? *Science*, **302**, 826–830.
65. Kaufmann, W.E. and Moser, H.W. (2000) Dendritic anomalies in disorders associated with mental retardation. *Cereb. Cortex*, **10**, 981–991.
66. Beites, C.L., Xie, H., Bowser, R. and Trimble, W.S. (1999) The septin CDCrel-1 binds syntaxin and inhibits exocytosis. *Nat. Neurosci.*, **2**, 434–439.
67. Yang, Y.M., Fedchyshyn, M.J., Grande, G., Aitoubah, J., Tsang, C.W., Xie, H., Ackerley, C.A., Trimble, W.S. and Wang, L.Y. (2010) Septins regulate developmental switching from microdomain to nanodomain coupling of Ca(2+) influx to neurotransmitter release at a central synapse. *Neuron*, **67**, 100–115.
68. Dong, Z., Ferger, B., Paterna, J.C., Vogel, D., Furler, S., Osinde, M., Feldon, J. and Bueler, H. (2003) Dopamine-dependent neurodegeneration in rats induced by viral vector-mediated overexpression of the parkin target protein, CDCrel-1. *Proc. Natl Acad. Sci. USA*, **100**, 12438–12443.
69. Tada, T., Simonetta, A., Batterton, M., Kinoshita, M., Edbauer, D. and Sheng, M. (2007) Role of Septin cytoskeleton in spine morphogenesis and dendrite development in neurons. *Curr. Biol.*, **17**, 1752–1758.
70. Tsang, C.W., Estey, M.P., Diciccio, J.E., Xie, H., Patterson, D. and Trimble, W.S. (2011) Characterization of presynaptic septin complexes in mammalian hippocampal neurons. *Biol. Chem.*, **392**, 739–749.
71. Ramocki, M.B. and Zoghbi, H.Y. (2008) Failure of neuronal homeostasis results in common neuropsychiatric phenotypes. *Nature*, **455**, 912–918.
72. Peng, X.R., Jia, Z., Zhang, Y., Ware, J. and Trimble, W.S. (2002) The septin CDCrel-1 is dispensable for normal development and neurotransmitter release. *Mol. Cell. Biol.*, **22**, 378–387.
73. Suzuki, G., Harper, K.M., Hiramoto, T., Funke, B., Lee, M., Kang, G., Buell, M., Geyer, M.A., Kucherlapati, R., Morrow, B. *et al.* (2009) Over-expression of a human chromosome 22q11.2 segment including TXNRD2, COMT, and ARVCF developmentally affects incentive learning and working memory in mice. *Hum. Mol. Genet.*, **18**, 3914–3925.
74. Zhu, H., Lee, M., Agatsuma, S. and Hiroi, N. (2007) Pleiotropic impact of constitutive fosB inactivation on nicotine-induced behavioral alterations and stress-related traits in mice. *Hum. Mol. Genet.*, **16**, 820–836.
75. Agatsuma, S., Lee, M., Zhu, H., Chen, K., Shih, J.C., Seif, I. and Hiroi, N. (2006) Monoamine oxidase A knockout mice exhibit impaired nicotine preference but normal responses to novel stimuli. *Hum. Mol. Genet.*, **15**, 2721–2731.
76. McIlwain, K.L., Merriweather, M.Y., Yuva-Paylor, L.A. and Paylor, R. (2001) The use of behavioral test batteries: effects of training history. *Physiol. Behav.*, **73**, 705–717.
77. Asada, A., Takahashi, J., Taniguchi, M., Yamamoto, H., Kimura, T., Saito, T. and Hisanaga, S. (2010) Neuronal expression of two isoforms of mouse Septin 5. *J. Neurosci. Res.*, **88**, 1309–1316.
78. Nathanson, J.L., Yanagawa, Y., Obata, K. and Callaway, E.M. (2009) Preferential labeling of inhibitory and excitatory cortical neurons by endogenous tropism of adeno-associated virus and lentivirus vectors. *Neuroscience*, **161**, 441–450.
79. Follenzi, A. and Naldini, L. (2002) HIV-based vectors. Preparation and use. *Methods Mol. Med.*, **69**, 259–274.
80. Hiroi, N. (1995) Compartmental organization of calretinin in the rat striatum. *Neurosci. Lett.*, **197**, 223–226.
81. Hiroi, N. and Graybiel, A.M. (1996) Atypical and typical neuroleptic treatments induce distinct programs of transcription factor expression in the striatum. *J. Comp. Neurol.*, **374**, 70–83.
82. Xu, M., Moratalla, R., Gold, L.H., Hiroi, N., Koob, G.F., Graybiel, A.M. and Tonegawa, S. (1994) Dopamine D1 receptor mutant mice are deficient in striatal expression of dynorphin and in dopamine-mediated behavioral responses. *Cell*, **79**, 729–742.

Citation: Transl Psychiatry (2012) 2, e146, doi:10.1038/tp.2012.70

www.nature.com/tp

Selective overexpression of *Comt* in prefrontal cortex rescues schizophrenia-like phenotypes in a mouse model of 22q11 deletion syndrome

S Kimoto[1,2,5], K Muraki[1,5], M Toritsuka[1,2,5], S Mugikura[3], K Kajiwara[3], T Kishimoto[2], E Illingworth[4] and K Tanigaki[1]

The 22q11.2 microdeletion is one of the highest genetic risk factors for schizophrenia. It is not well understood which interactions of deleted genes in 22q11.2 regions are responsible for the pathogenesis of schizophrenia, but *catechol-O-methytransferase* (*COMT*) is among the candidates. *Df1/+* mice are 22q11.2 deletion syndrome (22q11DS) model mice with a hemizygous deletion of 18 genes in the 22q11-related region. *Df1/+* mice showed enhanced response to the dopamine D1 agonist, SKF38393, and the *N*-methyl-D-aspartate antagonist, MK801, which can be normalized by a $GABA_A$ receptor agonist, bretazenil, or a $GABA_A$ $\alpha2/\alpha3$ receptor agonist, SL651498. Here, we demonstrated the curing effects of virus-mediated reintroduction of *Comt* to the prefrontal cortex (PFC) in *Df1/+* mice. In contrast, both *Comt* overexpression and Comt inhibition caused an abnormal responsiveness to Bretazenil, a $GABA_A$ receptor agonist in control mice. *Comt* overexpression increased MK801-induced interneuronal activation and GABA release in the PFC. The expression levels of GABA-related genes such as *Gabrb2* (*$GABA_A$receptor β2*), *Gad2* (glutamic acid decarboxylase 65 (*Gad65*)) and *Reln* (*Reelin*) correlate with a *Comt* expression level in PFC. Our data suggest that *Comt*-mediated regulation of GABAergic system might be involved in the behavioral pathogenesis of *Df1/+* mice.

Translational Psychiatry (2012) **2**, e146; doi:10.1038/tp.2012.70; published online 7 August 2012

Introduction

The 22q11.2 deletion syndrome (22q11DS) is known to be one of the highest risk factors for developing schizophrenia, and approximately one-fourth of 22q11DS patients develop schizophrenia.[1–3] All of the genes, except for one gene in human 22q11.2 region, exist on mouse chromosome 16.[4] Mice with a hemizygous deletion of 22q11.2-related region show schizophrenia-related behavioral abnormalities such as working memory deficits and sensory information-processing deficits.[5,6] These animal models of 22q11DS provide an opportunity to explore possible therapeutic strategies for this specific subtype of schizophrenia. The 22q11.2 deletion contains 35 known genes at least. However, it is not known which of these genes are responsible for the psychiatric disorders of 22q11DS. The cumulative effects of the deletion of more than one gene might be responsible for the increased risk for schizophrenia of 22q11.2 DS. An epistatic interaction between two genes in 22q11.2 region, *proline dehydrogenase* (*Prodh*) and *catechol-O-methyltransferase* (*Comt*), has been reported.[7] Pharmacological inhibition of Comt activity exacerbates behavioral abnormalities of *Prodh* knockdown mice.[7]

Comt is an enzyme that methylates catechol structures of dopamine (DA), norepinephrine (NE), caffeine and catechol estrogens. Comt plays a pivotal role in DA metabolism, specifically in the prefrontal cortex (PFC), because DA transporter is expressed in other brain regions, such as a striatum, and eliminates released DA even in the absence of Comt.[8,9] In *Comt* knockout (KO) male mice, two- to three-fold increases in DA were observed specifically in the PFC but not in other brain regions, and NE levels were not affected,[10] because the NE transporter is abundant in the PFC.[11,12] Administration of tolcapone, a specific brain-penetrant COMT inhibitor, causes an accumulation of 3,4-dihydroxy-phenylacetic acid (DOPAC) but has no effect on extracellular DA and NE, specifically in the PFC.[13]

Human genetic studies of functional polymorphisms of *Comt* such as $Val^{158}Met$ have suggested that deficiency in COMT activity might reduce cognitive function and cause psychiatric symptoms in 22q11DS,[14–17] although other studies have reported controversial results.[18–20] This might be caused by U-shaped effects of PFC DA level on cognitive functions.[21,22] Animal model studies using *COMT*-overexpressing transgenic mice and *Comt* KO mice have confirmed these complex effects of PFC DA levels, and have shown that either too little or too much DA in the PFC has impaired the PFC functions such as working memory and recognition memory.[23]

Comt is known to be also expressed in embryonic mouse brain,[24] and DA receptor KO mice show abnormal morphology of dendrites of PFC projection neurons, increased parvalbumin expression in PFC interneurons and reduced

[1]Research Institute, Shiga Medical Center, Moriyama, Shiga, Japan; [2]Department of Psychiatry, Nara Medical University Faculty of Medicine, Kashihara, Nara, Japan; [3]Division of Basic Medical Science and Molecular Medicine, School of Medicine, Tokai University, Isehara, Kanagawa, Japan and [4]University of Salerno, Fisciano, Italy
Correspondence: Dr K Tanigaki, Research Institute, Shiga Medical Center, Moriyama 5-4-30, Moriyama, Shiga 524-8524, Japan.
E-mail: tanigaki@res.med.shiga-pref.jp
[5]These authors contributed equally to this work.
Keywords: Comt; 22q11 deletion syndrome; interneuron; mouse models; schizophrenia
Received 8 December 2011; revised 21 May 2012; accepted 31 May 2012

mesencephalic dopaminergic neurons.[25,26] These data might suggest a possibility that Comt affects working memory and recognition memory through the regulation of neurodevelopmental process. To address whether adult functions of Comt is responsible for behavioral defects in *Df1/+* mice, one of 22q11DS model mice,[5] we examined the therapeutic potential of lentivirus-mediated *Comt* overexpression in the adult PFC of *Df1/+* mice.

Materials and methods

Generation and genotyping of *Dgcr2* KO mice. *Dgcr2* genomic fragments were cloned by screening of a phage library containing 129/Sv mouse DNA fragment. To construct a targeting with a 5.6-kb 5′-recombinogenic arm and a 1.2-kb 3′-recombinogenic arm, EGFP-SV40-polyA—a neomycin phosphotransferase-expressing cassette (EGFP-Neo) — was inserted between *Sma*I and *Xho*I in exon 1 to replace the region between the two restriction sites. A dyphtheria toxin A-expressing cassette was flanked outside the 3′ homologous region. The vector was linearized by restriction digestion and used to transfect embryonic stem cell line E14 by electroporation. Transfected cells were cultured in the presence of G418. Upon successful targeting, the neomycin expression cassette replaced exon 1 and the initiation codon of all the transcripts of *Dgcr2*. Therefore, it is expected to disrupt all *Dgcr2* transcripts (Figure 2). Correct targeting through homologous recombination in embryonic stem cells was confirmed by PCR and Southern blot. PCR for the KO allele was performed using the following primers: wild-type forward primer 5′-TTCCTGCTGGTTCTCACTGT-3′, reverse primer 5′-TCAAGGTCCCATTACTCCCTC-3′ and neo primer 5′-TATTGCTGAAGAGCTTGGCG-3′. The wild-type allele produces a 1.6-kb band, whereas the targeted allele produces a 1.4-kb band. For Southern blotting, isolated genomic DNA was digested with *Eco*RI. The 7.5 and 5.8 kb fragments corresponding to the wild-type and KO allele were identified by hybridization with the 5′ internal probe (Probe A, Figure 2b).

Animals. Generation of *Df1/+* 22q11DS model mice was previously described in detail.[5,27] Mice were maintained on the C57Bl/6 genetic background for at least 11 generations. Male, 2–3-month-old mice were used for behavioral analysis. Mouse colonies were maintained in accordance with the protocols approved by the Committee on Animal Research at Research Institute, Shiga Medical Center.

Reverse transcription PCR (RT PCR) analysis. The following primers were used to amplify target: *Dgcr2*; 5′-TTCCTGC TGGTTCTCACTG-3′ and 5′-GTGGAGAAGGTAGCAAGT GA-3′; β-actin; and Mouse β-Actin Control Amplimer Set (Clontech, Mountain View, CA, USA).

Cloning and production of lentiviral vectors. Cytomegalovirus (CMV)-IE/chicken β-actin promoter (CAG), 1.6-kb fragment cut from pXCAG, mouse α-calcium/calmodulin-dependent protein kinase II (CaMKII) promoter 1.2-kb fragment and mouse membrane-bound-type *Comt* were introduced to FUGW lentiviral vector and lentiviruses were produced as previously described.[28] Briefly, human embryonic kidney 293T cells were transfected by using the Lipofectamine 2000 (Invitrogen, Tokyo, Japan) with the lentiviral vector and two helper plasmids, Δ8.9 and VSVG. After 48 h, the supernatants were spun at 780 × *g* for 5 min, filtered through a 0.45 μm pore size filter (Millipore, Billerica, MA, USA) to remove cell debris, spun at 83 000 × *g* for 1.5 h, and the pellet was resuspended in 100 μl of phosphate-buffered saline. For virus titration, HEK293T cells were infected with lentiviruses in decreasing concentrations. At 72 h after infection, cells were fixed in 4% paraformaldehyde and lentivirus-mediated *Comt*/EGFP expression was estimated by immunofluorescent analysis. Concentrated lentiviral titers ranged from 1×10^8 to 1×10^9 transducing units (TU) per ml.

Stereotaxic surgery. Injections of lentiviruses were performed stereotaxically in 8- to 10-week-old mice.

Mice were anesthetized using 2.5% Avertin solution and stereotaxic surgery was performed under standard conditions. The coordinate of the injection site was 2.0 mm anterior and 0.70 mm lateral to bregma at a depth of 1.75 and 2.25 mm at an 8° angle, and 2.4 mm anterior and 0.50 mm lateral to bregma at a depth of 1.13 mm at an 8° angle. All procedures were performed according to the guidelines on animal experiments of Shiga Medical Center. A total of 0.5 μl of purified virus was delivered on each side over a 3-min period. Lentivirus-infected mice were used for experiments at least 2 weeks after surgical operations for recovery. For verification of injection sites, 30 μm thick sections were cut using a cryostat at the level of PFC. Lentivirus infection was verified by immunohistochemical analysis of Comt for Lenti-CAG Comt or Lenti-CaMKII-Comt vector, and EGFP for Lenti-CAG-GFP vector.

Open field test. Locomotor activity was measured in the open field activity chambers (40 × 40 × 40 cm) equipped with photocells (beam spacing 2.5 cm) for the automatic recording of horizontal and vertical activity. Stereotypy count was analyzed using the VersaMax system (Accuscan Instruments, Columbus, OH, USA). Stereotypy was recorded when the mouse broke the same beams repeatedly. Stereotypy count is the number of beam breaks during stereotypic activity. Data were collected for 60 min.

Quantification of prefrontal cortical catecholamines and their metabolites. The mice were decapitated 2 weeks after lentiviral infection and the brains were quickly removed. Wet prefrontal cortical tissues were homogenized in two volumes of 0.2 M perchloric acid buffer containing 100 μM EDTA 2Na and 1 μg ml^{-1} isoproterenol as an internal standard (500 μl per 100 mg wet weight tissue) and kept on ice for 30 min. Homogenates were centrifuged at 15 000 r.p.m. for 15 min at 4 °C. The supernatants were collected, adjusted to pH 3 with 3M CH_3COONa and analyzed by the high-performance liquid chromatography system with an electrochemical detector (HTEC-500, Eicom, Kyoto, Japan) for the analysis of DA, DOPAC, homovanillic acid (HVA), serotonin and 5-hydroxyindoleacetic acid (5-HIAA). The column used for separation was a SC-5ODS (Eicom). The mobile phase was

0.1 M sodium phosphate buffer (0.1 M NaH2PO4:0.1 M Na2HPO4 = 1000:160, v/v), 1% methanol, 500 mg l^{-1} sodium sulfonate, and 50 mg l^{-1} EDTA.

Cannula implantation. The mice were anesthetized with 2.5% Avertin solution and stereotaxic surgery was performed under standard conditions. The guide cannula (AG-2, Eicom) with length 2 mm, inner diameter 0.4 mm and outer diameter 0.5 mm was implanted into the PFC (A +2.2 mm, L 0.5 mm and V 1 mm from the bregma) and fixed to the skull with dental cement. Following surgery, the animals were returned to their home cage and allowed to recover for 1 day before beginning of the experiment.

Microdialysis and high-performance liquid chromatography analysis. The microdialysis probe (A-1-4-02, Eicom) with an active dialysis membrane (2 mm long, i.d. 0.20 mm, o.d. 0.22 mm, cut-off value 50 kDa) was inserted carefully into the PFC. The implanted microdialysis probe was connected to a 2.5 ml gastight syringe (Hamilton, Tokyo, Japan) and perfused with Ringer's solution (147 mM NaCl, 4 mM KCl and 2.3 mM $CaCl_2$) at a constant flow of 1 ml min^{-1} using a microperfusion pump (ESP-32, Eicom) via a swivel system (Eicom), allowing the mice to move freely in a Plexiglas box (30 cm × 30 cm × 40 cm). The dialysate collected for the first 2 h was discarded to ensure a stable baseline of DA and γ-aminobutyric acid (GABA) release.

The DA content in the dialysate was quantified in the same way as for tissue homogenates. GABA content in the dialysate was quantified by high-performance liquid chromatography with electrochemical detector after derivatization of the amino acids with *o*-phthaldialdehyde (OPA) and 2-mercaptoethanol solution (Eicom). A total of 20 µl samples of perfusate were collected at 20 min intervals. One volume (5 ml) of 4 mM OPA was added to three volumes of dialysate and allowed to react for 2.5 min at room temperature. Then, the sample of the perfusate/OPA solution was injected into the high-performance liquid chromatography/electrochemical detector with a graphite electrode set at 600 mV against an Ag/AgCl reference electrode (Eicom). GABA was separated on SC-5 ODS column (2.1 mm × 150 mm, Eicom). The mobile phase consisted of 0.1 M phosphate buffer, 0.013 mM EDTA 2Na, pH 6.0, with 30% MeOH pumped at a flow rate of 0.23 ml min^{-1}. The basal output was defined as the average of three samples before drug administration. The results were calculated as percentage of the baseline output of DA and GABA.

Immunohistochemical analysis. Mice were injected with MK801 (0.32 mg kg^{-1}) intraperitoneally (i.p.) 2 h before killing for immunohistochemical analysis of c-Fos staining. Mice were perfused transcardially by 4% paraformaldehyde and 0.05% glutalaldehyde. The serial 30 µm cryostat sections were incubated with primary antibodies for 24 h at 4 °C after blocking for 30 min at room temperature with 5% donkey serum (Chemicon, Temecula, CA, USA) and for 1 h at room temperature with secondary antibodies (Molecular Probes, Eugene, OR, USA, and Vector Labs, Burlingame, CA, USA). The primary antibodies used were anti-Comt (Santa Cruz, Santa Cruz, CA, USA), anti-S100β (Sigma-Aldrich, St Louis, MO, USA), anti-NeuN (Chemicon), anti-c-Fos (Ab5, Calbiochem, San Diego, CA, USA), anti-GABA (GB69, Sigma-Aldrich) and anti-Gad67 (Chemicon). Peroxidase activity was visualized by Vectastatin Elite ABC Kit (Vector Labs). Slides were examined with a Zeiss microscope (Axiovert200M) (Zeiss, Tokyo, Japan) or an Olympus confocal laser scanning microscope (FV-300, Olympus, Tokyo, Japan). For the quantification of c-Fos-positive cells, the locations of prelimbic cortices of the PFC were defined according to the mouse brain in stereotaxic coordinates (2001, Academic Press, San Diego, CA, USA). The c-Fos-immunoreactive cells in the regions of interest were counted bilaterally in four serial sections matched for rostocaudal level by bregma distance per mice. For the quantification of Gad67 and GABA immunofluorescence, the perisomatic (puncta rings) or neuropil areas were delineated and then pixel density within the delineated area was calculated and averaged as described previously. At least four sections from four mice were analyzed.

Quantitative RT-PCR. Complementary DNA was obtained using a PrimeScript 1st strand cDNA synthesis kit (Takara, Shiga, Japan). Intron spanning *Taq*man probes were designed using the Roche Universal Probe Library method. Amplifications were run in a LightCycler 480 system (Roche, Tokyo, Japan). All data were analyzed using glyceraldehyde-3-phosphate dehydrogenase (GAPDH) levels as reference.

The following primers were employed: *Gabrb2*, 5′-CGAT GGCACTGTCCTGTATG-3′ and 5′-ATACCGCCTTAGGTCC ATCA-3′, probe: human #27; *Gad2*: 5′-TCAACTACGC GTTTCTGCAC-3′ and 5′-AGAGTGGGCCTTTCTCCATC-3′, probe: human #62; *Reln*: 5′-CGTGCTGCTGGACTTCTCT-3′ and 5′-TCCATCTCGTGAAGCAAGGT-3′, probe: human #58; *Comt*: 5′-CTCGGGGTCAGACCTGTG-3′ and 5′-GCAACAG GAGACCCAATGA-3′, probe: human #66.

Results

Enhanced responsiveness to MK801 of *Df1/+* mice was normalized by $GABA_A$ receptor agonists. The DA agonists and *N*-methyl-D-aspartate receptor (NMDAR) antagonists such as Dizocilpine (MK801) are known to have psychometric effects on healthy individuals, and exacerbate symptoms of schizophrenia patients.[29–31] In *Df1/+* mice, the locomotor response to MK801 treatment (0.32 mg kg^{-1}) was significantly enhanced (genotype-by-time interaction on the distance traveled, $F_{11,165} = 5.60$, $n = 6–11$ per group, $P < 0.0001$ (repeated two-way analysis of variance (ANOVA); Figure 1a). One of the primary pathologies observed in schizophrenia is a deficit in GABA signaling.[32–34] At first, to investigate a possible involvement of GABA signaling in the behavioral abnormality of *Df1/+* mice, we examined the effect of a nonselective $GABA_A$ partial receptor agonist, bretazenil. Bretazenil at 10 mg kg^{-1} normalized the enhanced response of *Df1/+* mice to MK801 (*Df1/+* mice: MK801 and bretazenil treatment; 4553.00 ± 1307.28 cm, MK801 treatment; 10825.50 ± 1372.96 cm, $n = 6–7$ per group, $P = 0.0071$; Figures 1a–c). In contrast, in control mice, bretazenil had no effect on the traveled distance during 60 min after administration (control mice: MK801 and

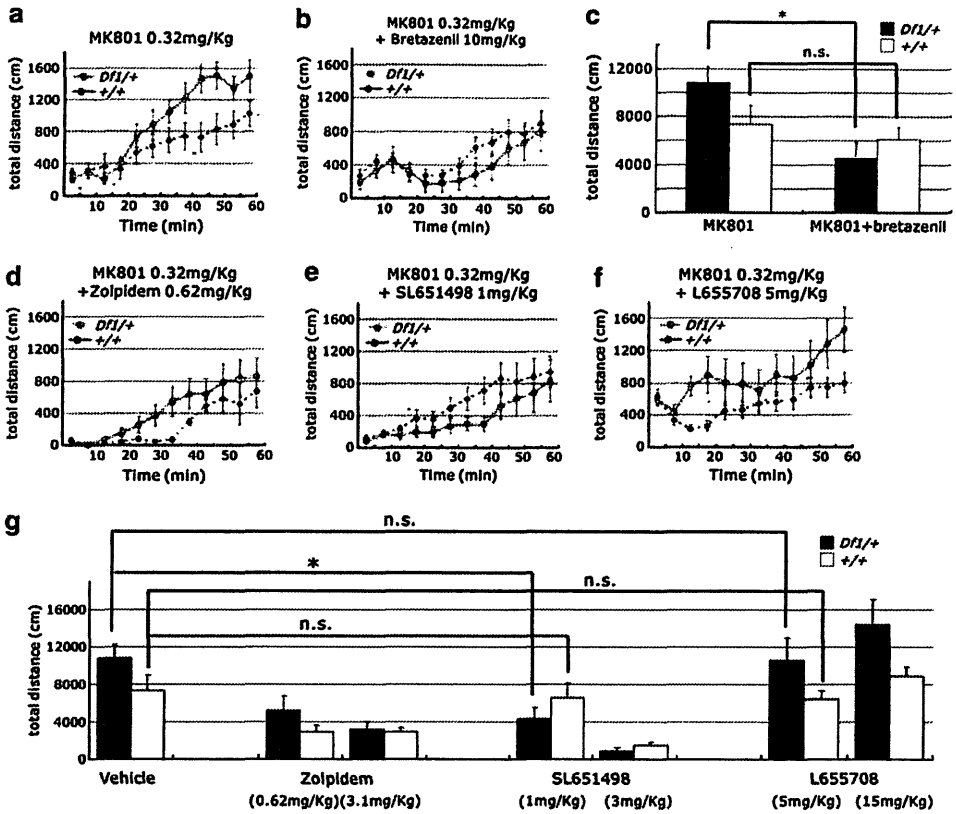

Figure 1 Enhanced responsiveness of *Df1/+* mice to MK801 is reversed by $GABA_A$ α2/α3 receptor agonist, SL651498. (**a–c**) Enhanced response of male *Df1/+* mice to MK801 (**a**, **c**). Bretazenil attenuated enhanced locomotion of *Df1/+* mice by MK801 (**b**, **c**). MK801 (0.32 mg kg^{-1}) was intraperitoneally injected (**b**) with or (**a**) without bretazenil (10 mg kg^{-1}). Ambulatory distance is shown in 5 min bins for 60 min after drug administration (**a**, **b**) and quantification of ambulatory distance for 60 min is shown in (**c**). Values are the mean ± s.e.m. for 6–16 male mice. $^*P = 00071$; NS, not significant. (**d–g**) SL651498 (**e**), but neither zolpidem (**d**) nor L655708 (**f**), attenuated enhanced locomotion of *Df1/+* mice by MK801. MK801 (0.32 mg kg^{-1}) was intraperitoneally injected to male *Df1/+* and control mice with Zolpidem (0.62 or 3.1 mg kg^{-1}) (**d**, **g**), SL651498 (1 or 3 mg kg^{-1}) (**e**, **g**) and L655708 (5 or 15 mg kg^{-1}) (**f**, **g**). Ambulatory distance is shown in 5 min bins for 60 min after drug administration (**e–g**) and quantification of ambulatory distance for 60 min is shown in (**g**). Values are the mean ± s.e.m. for 6–16 male mice. $^*P = 0.0043$.

bretazenil treatment; 6092.63 ± 1026.79 cm, MK801 treatment; 7359.18 ± 1586.83 cm, $n = 11–16$ per group, $P = 0.97$; Figures 1a–c). Next, to analyze which type of $GABA_A$ receptor is responsible for this reversing effect of bretazenil, *Df1/+* mice were treated with selective GABA agonists. SL651498, a selective agonist of $GABA_A$ α2/α3 receptor, but neither zolpidem, a selective agonist of $GABA_A$ α1 receptor, nor L655708, a selective inverse agonist of $GABA_A$ α5 receptor, specifically reversed the enhanced response of *Df1/+* mice to MK801 (ambulatory distance for 60 min after administration of drugs: control mice; MK801 and SL651498 1 mg kg^{-1} treatment, 6580.75 ± 1499.15 cm, MK801 treatment, 7359.18 ± 1586.83 cm, $n = 8–11$ per group, $P = 0.73$, *Df1/+* mice; MK801 and SL651498 1 mg kg^{-1} treatment, 4332.44 ± 1229.75 cm, MK801 treatment, 10 825.50 ± 1372.96 cm, $n = 6–9$ per group, $P = 0.0043$; Figures 1d–g). Taken together, our data demonstrated that *Df1/+* mice show high responsiveness to MK801 like human schizophrenic patients, and the GABAergic transmission through $GABA_A$ α2/α3 receptor may be involved in this abnormal behavioral phenotype of *Df1/+* mice.

However, the deleted region of *Df1/+* mice is smaller than 1.5-Mb deletion found in human 22q11DS, which does not include *Dgcr2* (Figure 2a). Recently, it has been reported that a potentially destructive *de-novo* mutation was found in *Dgcr2* in a human schizophrenic patient,[35] which suggests a possible involvement of *Dgcr2* in the pathogenesis of schizophrenia. To examine whether or not *Dgcr2* haplodeletion also causes behavioral abnormalities similar to that in *Df1/+* mice, we genetically engineered *Dgcr2* KO mice by homologous recombination in embryonic stem cells. To introduce a targeted mutation in the mouse *Dgcr2* gene, we constructed a targeting vector, in which the expression cassette of EGFP-SV40 polyA and the *neomycin resistance* (EGFP-*Neo*) gene was inserted in exon 1, which contains an initiation codon of *Dgcr2* and flanked by the 5′ 5.6-kb and 3′ 1.2-kb *Dgcr2* gene fragments (Figure 2b). This mutation is predicted to introduce a premature stop codon to all the transcripts of *Dgcr2*. The disrupted *Dgcr2* allele was confirmed by Southern blot analysis (Figure 2c) and genomic PCR (data not shown). $Dgcr2^{-/-}$ mice were backcrossed to the C57BL/6 for 10 generations before behavioral analysis. No *Dgcr2* RNA transcript could be detected by RT-PCR in the brains of the mutant mice, validating *Dgcr2* genetic disruption (Figure 2d). $Dgcr2^{-/-}$ mice were born according to Mendelian segregation, were viable and fertile, and visually indistinguishable from their wild-type littermates. Histopathological

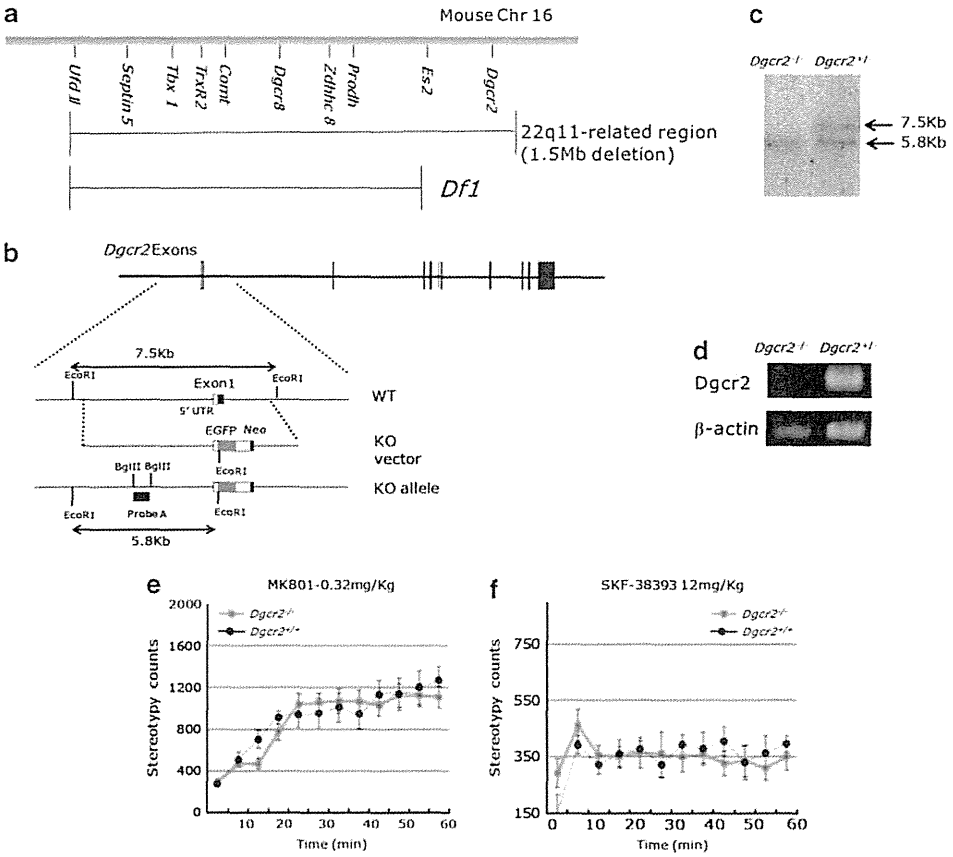

Figure 2 Normal responses of *Dgcr2* knockout (KO) heterozygous mice to MK801 and SKF38393. (**a**) A genetic organization of mouse 22q11-related region on chromosome 16 (Chr 16). The deleted region of *Df1/+* mice is indicated by a line below the map. (**b**) Schematic representation of *Dgcr2* gene-targeting strategy. Exon 1 was replaced by a EGFP-Neo cassette by homologous recombination, which is predicted to introduce a premature stop codon in all *Dgcr2* transcripts. UTR, untranslated region; WT, wild type. (**c**) Southern blot analysis of genomic DNA using probe A is shown in (**b**). The 7.5 and 5.8 kb *Eco*RI fragments derived from the wild-type and *Dgcr2* KO mice, respectively. (**d**) RT-PCR analysis of *Dgcr2* in the brain. (**e**, **f**) *Dgcr2* heterozygosity did not affect the locomotor responses to MK801 and SKF38393. (**e**) MK801 (0.32 mg kg^{-1}) and (**f**) SKF38393 (12 mg kg^{-1}) were injected intraperitoneally and subcutaneously, respectively, to the *Dgcr2*$^{-/-}$ and control mice. Stereotypy count is shown in 5 min bins for 60 min after drug administration. Values are the mean ± s.e.m. for 6–14 male mice.

analysis did not show any abnormality of gross morphology in the brains of *Dgcr2* KO mice (data not shown). In an open field test, *Dgcr2* KO heterozygous mice did not show any abnormalities in the locomotor responses to MK801 (0.32 mg kg^{-1}, i.p.) and D1 agonist, SKF38393 (12 mg kg^{-1}, subcutaneously; genotype-by-time interaction on the stereotypy count, MK801; $F_{11,253}=1.14$, $n=11$–14 per group, $P=0.33$, SKF38393; $F_{11,\ 110}=1.18$, $n=5$–7 per group, $P=0.31$ (repeated two-way ANOVA; Figures 2e and f). Therefore, we adopted *Df1/+* mice for further analysis.

Prefrontal cortical gene transfer of *Comt* in *Df1/+* mice. To examine whether the reduced expression of *Comt* is involved in behavioral defects of *Df1/+* mice, we bilaterally reintroduce mouse *Comt* to the prelimbic cortex and the infralimbic cortex of *Df1/+* mice by stereotactic injection of lentiviruses, using EGFP as a control (Figure 3a). To distinguish cell type-specific effects of *Comt* overexpression, we utilized two types of lentivirus vectors, one of which is with a ubiquitous CMV/CAG promoter (Lenti-CAG-Comt)[36] and the other is with a neuron-specific CaMKII promoter (Lenti-CaMKII-Comt). Western blotting analysis showed that both membrane-bound and soluble forms of Comt were generated from the same mRNA derived from a lentivirus (Figure 3c). Lentivirus-mediated specific expression of *Comt* in the PFC was confirmed by immunohistochemical analysis (Figure 3b). Quantitative real-time PCR analysis showed that *Comt* expression reduced by 55% in the PFC of Df1 mice than that of control mice ($P=0.0000068$; Figure 3d). After Lenti-CAG-Comt infection, *Comt* expression increased to ~150% of that of EGFP-expressing control PFC in *Df1/+* mice (Figure 3d). Immunofluorescent study showed that in Lenti-CAG-Comt-infected PFC, 19.43 ± 1.63% of *Comt*-expressing cells were S100β-positive glial cells and 55.66 ± 2.26% were NeuN-positive neurons, and 4.71 ± 1.94% were Gad67-positive interneurons ($n=6$), whereas in Lenti-CamKII-Comt-infected PFC, 1.99 ± 1.11% of *Comt*-expressing cells were S100β-positive glial cells and 89.27 ± 2.21% were NeuN-positive neurons, and 15.69 ± 1.18% were Gad67-positive interneurons ($n=3$; Figure 3g). The percentage of Lenti-CamKII-Comt-transduced interneurons was 4 times higher than that observed with Lenti-CAG-Comt lentivirus.

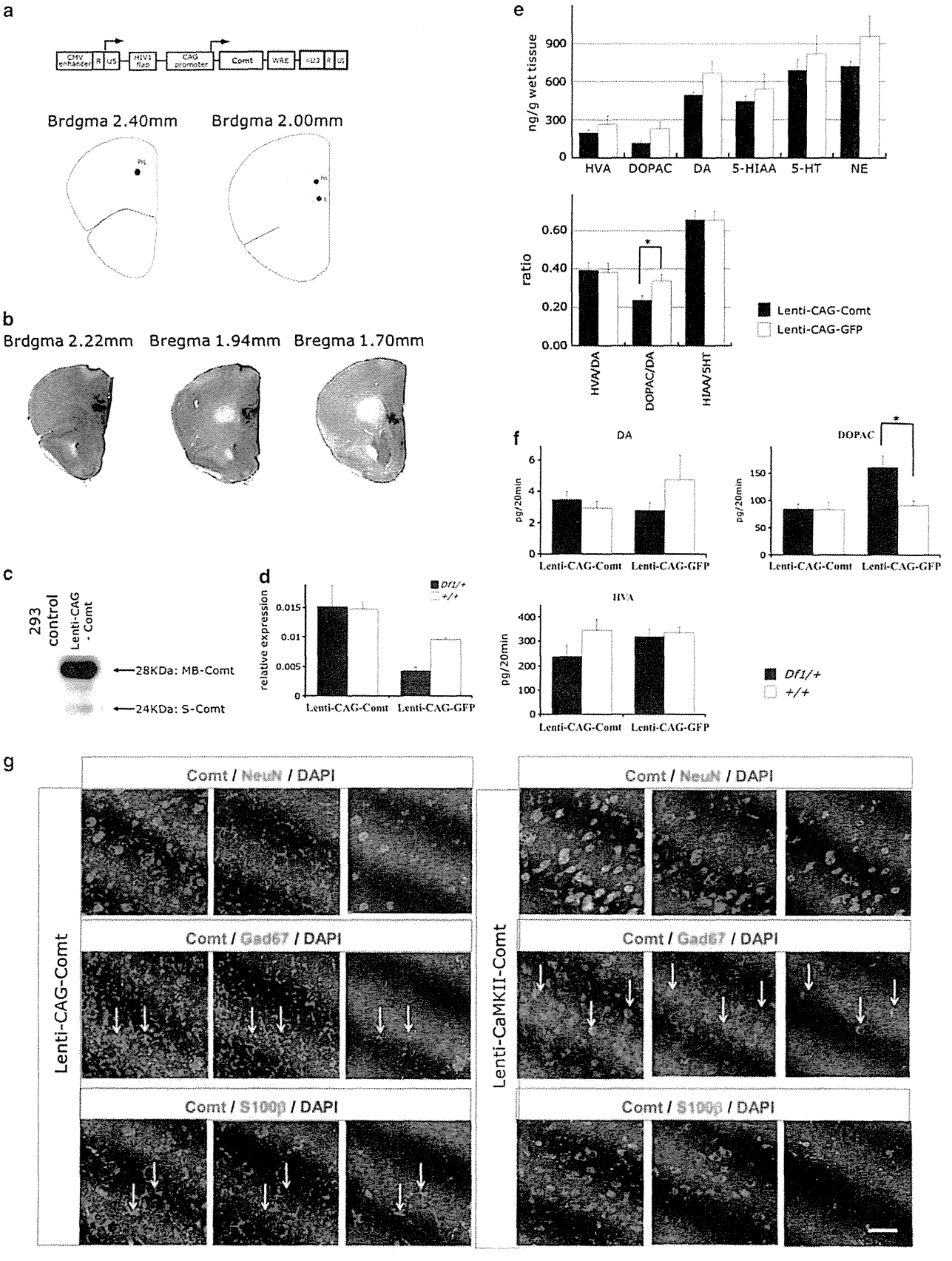
a
CMV enhancer
R
U5
HIV1 flap
CAG promoter
Comt
WRE
ΔU3
R
U5
Brdgma 2.40mm
Brdgma 2.00mm
b
Brdgma 2.22mm
Bregma 1.94mm
Bregma 1.70mm
c
293 control
Lenti-CAG - Comt
28KDa: MB-Comt
24KDa: S-Comt
d
relative expression
Df1/+
+/+
Lenti-CAG-Comt
Lenti-CAG-GFP
e
ng/g wet tissue
HVA
DOPAC
DA
5-HIAA
5-HT
NE
ratio
HVA/DA
DOPAC/DA
HIAA/5HT
Lenti-CAG-Comt
Lenti-CAG-GFP
f
DA
DOPAC
HVA
pg/20min
Df1/+
+/+
g
Comt / NeuN / DAPI
Comt / Gad67 / DAPI
Comt / S100β / DAPI
Lenti-CAG-Comt
Lenti-CaMKII-Comt

To determine whether the lentivirus-derived Comt was functional *in vivo*, we examined DA and DA metabolites in homogenates of lentivirus-infected prefrontal cortical tissues. Comt methylates DOPAC, a hydroxylated metabolite of DA, as well as DA and forms HVA. The ratio of DOPAC/DA significantly decreased by the overexpression of *Comt* in the PFC, whereas neither HVA/DA nor HIAA/5HT ratio was affected (HVA: Lenti-CAG-GFP; $265.18 \pm 67.16\,ng\,g^{-1}$, Lenti-CAG-Comt; $195.97 \pm 23.91\,ng\,g^{-1}$, $P=0.32$, DOPAC: Lenti-CAG-GFP; $229.36 \pm 54.58\,ng\,g^{-1}$, Lenti-CAG-Comt; $117.52 \pm 14.93\,ng\,g^{-1}$, $P=0.06$, DA: Lenti-CAG-GFP; $665.51 \pm 93.78\,ng\,g^{-1}$, Lenti-CAG-Comt; $495.09 \pm 23.34\,ng\,g^{-1}$, $P=0.090$, 5-HIAA: Lenti-CAG-GFP; $543.19 \pm 118.03\,ng\,g^{-1}$, Lenti-CAG-Comt; $445.18 \pm 41.47\,ng\,g^{-1}$, $P=0.42$, 5-HT: Lenti-CAG-GFP; $816.30 \pm 146.01\,ng\,g^{-1}$, Lenti-CAG-Comt; $691.61 \pm 84.22\,ng\,g^{-1}$, $P=0.46$, NE: Lenti-CAG-GFP; $957.29 \pm 160.62\,ng\,g^{-1}$, Lenti-CAG-Comt; $723.92 \pm 35.97\,ng\,g^{-1}$, $P=0.16$, HVA/DA: Lenti-CAG-GFP; 0.38 ± 0.049, Lenti-CAG-Comt; 0.39 ± 0.040, $P=0.86$, DOPAC/DA: Lenti-CAG-GFP; 0.34 ± 0.035, Lenti-CAG-Comt; 0.24 ± 0.026, $P=0.048$, HIAA/5HT: Lenti-CAG-GFP; 0.66 ± 0.049, Lenti-CAG-Comt; 0.66 ± 0.047, $P=0.98$; Figure 3e), indicating that *Comt* overexpression can enhance elimination of DA and DOPAC in the PFC in wild-type mice. Finally, we examined whether lentivirus-mediated *Comt* overexpression can compensate for the effects of *Comt* heterozygosity of *Df1/+* mice by *in vivo* microdialysis. In *Df1/+* mice, PFC extracellular DOPAC levels increased by 77.89%, and there were no changes in DA and HVA levels (DOPAC: *Df1/+* Lenti-CAG-GFP; 160.97 ± 21.85 pg per 20 min, *+/+* Lenti-CAG-GFP; 90.49 ± 9.89, $P=0.0041$, DA: *Df1/+* Lenti-CAG-GFP; 2.80 ± 0.34 pg per 20 min, *+/+* Lenti-CAG-GFP; 4.75 ± 1.56, $P=0.42$, HVA: *Df1/+* Lenti-CAG-GFP; 319.96 ± 30.15 pg per 20 min, *+/+* Lenti-CAG-GFP; 336.29 ± 22.97, $P=0.69$; Figure 3f). Lenti-CAG-Comt-mediated *Comt* overexpression successfully normalized the PFC extracellular DOPAC level in *Df1/+* mice (DOPAC: *Df1/+* Lenti-CAG-Comt; 84.74 ± 8.99 pg per 20 min, *+/+* Lenti-CAG-GFP; 90.49 ± 9.89 pg per 20 min, $P=0.78$; Figure 3f).

***Comt* overexpression in the PFC reversed behavioral abnormalities of *Df1/+* mice.** PFC EGFP-expressed *Df1/+* mice showed a similar enhanced locomotor response to MK801 ($0.32\,mg\,kg^{-1}$, i.p.) and SKF38393 ($12\,mg\,kg^{-1}$, subcutaneously) as seen with non-lentivirus-infected *Df1/+* mice (stereotypy count for 60 min after administration, SKF38393: *+/+*; 4886.0 ± 725.1, *Df1/+*; 6066.4 ± 1227.3, $P=0.019$, MK801: *+/+*; $11\,647.1 \pm 4485.6$, *Df1/+*; $16\,492.1 \pm 4305.0$, $P=0.039$; Figures 4b and e). Increasing *Comt* expression levels by lentiviral infection normalized the enhanced sensitivity of *Df1/+* mice to MK801 and SKF38393, whereas it did not alter locomotor responses in control mice (stereotypy count of *Comt*-expressing lentivirus-infected mice for 60 min after administration, SKF38393: *+/+*; 5356.0 ± 1157.0, *Df1/+*; 4092.5 ± 1633.8, $P=0.047$, MK801: *+/+*; $15\,753.2 \pm 1509.0$, *Df1/+*; $12\,331.7 \pm 2409.6$, $P=0.019$; Figures 4a and d). Next, we investigated whether this treatment effect directly depends on Comt enzymatic activity or not. At first, we determined an optimal concentration of tolcapone, a Comt inhibitor by *in vivo* microdialysis experiments. We found that $30\,mg\,kg^{-1}$ tolcapone (i.p.) efficiently inhibited Comt activity in PFC, increased DOPAC level and decreased HVA level to a comparable level to that in control mice even in the Comt-overexpressed mice, whereas $6\,mg\,kg^{-1}$ tolcapone administration was not sufficient (Figure 5). Therefore, we adopted $30\,mg\,kg^{-1}$ tolcapone for further experiments. However, $30\,mg\,kg^{-1}$ of tolcapone failed to reverse the curing effects of PFC *Comt* overexpression. On the contrary, tolcapone administration of this dose even reduced the response of *Comt*-overexpressing *Df1/+* mice to MK801 but not to SKF38393 (MK801 + tolcapone: stereotypy count for 60 min after administration, *+/+*; $12\,092.0 \pm 5551.9$, *Df1/+*; 6433.5 ± 3121.1, $P=0.049$; Figures 4c and f), suggesting that the indirect effects of increased Comt enzymatic activity might be responsible for its curing potential.

***Comt* overexpression normalized the abnormal responsiveness of *Df1/+* mice to $GABA_A$ receptor agonists.** The enhanced response of EGFP-overexpressed *Df1/+* mice to MK801 or SKF38393 was also reversed by SL651498 administration as in non-virus-infected *Df1/+* mice (Figures 4b and e, and 6b and e). In addition, *Df1/+* mice showed an abnormal response to bretazenil when treated with methamphetamine ($1\,mg\,kg^{-1}$, i.p.; stereotypy count from 30 to 60 min after administration, *Df1/+* mice, methamphetamine, 4104.63 ± 565.90, methamphetamine + bretazenil 1984.60 ± 721.46 ($P=0.048$); Figure 7c). Next, we examined the effects of Lenti-CAG-Comt treatment on this GABAergic response abnormality of *Df1/+* mice. After

Figure 3 The gene delivery of *catechol-O-methytransferase* (*Comt*) to the prefrontal cortex (PFC). **(a)** Depiction of the lentivirus to locally overexpress *Comt* (upper panel). CMV enhancer is substituted for U3 region of the 5′ long terminal repeat (LTR) to enhance expression of viral RNA genomes. Self-inactivating 3′ LTR comprises a U3 region with deletion of an enhancer element (ΔU3). HIV-1-flap: the human immunodeficiency virus-1 flap element; WRE: the woodchuck hepatitis virus posttranslational regulatory element. Schematic illustration of injection sites in the PFC (lower panel). IrL, infralimbic cortex; PrL, prelibmic cortex. **(b)** Immunohistochemical studies for Comt expression in a representative mice bilaterally infected by Lenti-CAG-Comt, demonstrating spatial selectivity. **(c)** Western blot analysis of Comt expression. Protein samples from 293 cells 2 days after infection of Lenti-CAG-Comt. MB-Comt, membrane-bound Comt, S-Comt, soluble Comt. **(d)** Real-time PCR quantitation of *Comt* mRNA levels in Lenti-CAG-Comt- or Lenti-CAG-GFP-infected PFC of *Df1/+* or control mice. Results were normalized to glyceraldehyde-3-phosphate dehydrogenase (GAPDH) abundance. Data are the mean ± s.e.m. from 3 to 14 mice. $^*P=0.0000068$. **(e)** Effect of *Comt* overexpression on dopamine (DA), homovanillic acid (HVA), 3,4-dihydroxyphenylacetic acid (DOPAC), 5-hydroxytryptamine (5HT), 5-hydroxyindoleacetic acid (5-HIAA) and norepinephrine (NE) in tissue homogenates of the Lenti-CAG-Comt- or Lenti-CAG-GFP-infected PFC of control mice. Values are the mean ± s.e.m. for 4 mice. $^*P=0.048$. **(f)** Effects of *Comt* overexpression on PFC extracellular DA, DOPAC and HVA in the PFC of Lenti-CAG-Comt- or Lenti-CAG-GFP-infected *Df1/+* and control mice. The 20 min baseline fractions were collected after 2 h washout period. Data are means ± s.e.m. from 3 to 11 mice. $^*P=0.0041$. **(g)** Representative images of immunofluorescent studies of Lenti-CAG-Comt- or Lenti-CaMKII-Comt-infected PFC for Comt (green), NeuN (red, upper panels), S100β (red, lower panels) and 4′,6-diamidino-2-phenylindole (DAPI) staining of nuclei (blue). Double positive cells are indicated by arrows. Scale bar = 20 μm.

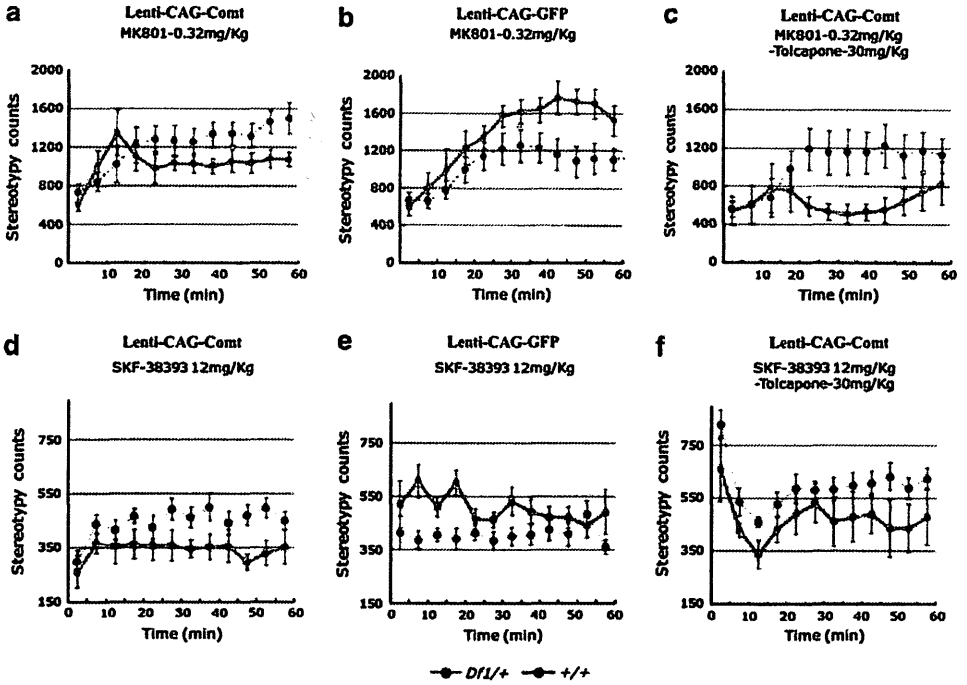

Figure 4 Increasing *catechol-O-methytransferase* (*Comt*) expression in the prefrontal cortex (PFC) rescues schizophrenia-like phenotypes of *Df1/+* mice. (**a**, **b**, **d**, **e**) Enhanced response of male *Df1/+* mice to MK801 (**b**) and SKF38393 (**e**) were normalized by lentivirus-mediated *Comt* overexpression in the PFC (**a**, **d**). SKF38393 (12 mg kg^{-1}) and MK801 (0.32 mg kg^{-1}) were injected subcutaneously and intraperitoneally, respectively, to the mice infected with Lenti-CAG-Comt (**a**, **d**) or control Lenti-CAG-GFP (**b**, **e**). Stereotypy count is shown in 5 min bins for 60 min after drug administration. Values are the mean ± s.e.m. for 6–16 male mice. (**c**, **f**) Tolcapone, a Comt inhibitor, failed to reverse a therapeutic effect of *Comt* overexpression of the enhanced stereotypic response of *Df1/+* mice to MK801 (**c**) and SKF38393 (**f**). Tolcapone (30 mg kg^{-1}) was intraperitoneally injected to male *Df1/+* mice 1 h before administration of MK801 (0.32 mg kg^{-1}). Stereotypy count is shown in 5 min bins for 60 min after MK801 administration. Values are the mean ± s.e.m. for 5–16 male mice.

lentivirus-mediated PFC *Comt* reintroduction, *Df1/+* mice showed reduced responses to SL651498 or bretazenil (stereotypy count for 60 min after administration, Lenti-CAG-GFP-infected *Df1/+* mice: MK801; 16492.13 ± 1435.01, MK801 + SL651498; 3321.75 ± 794.36 (P = 0.0000022), Lenti-CAG-Comt-infected *Df1/+* mice: MK801; 12331.71 ± 910.752, MK801 + SL651498; 8073.75 ± 1276.90 (P = 0.020), Lenti-CAG-GFP-infected *Df1/+* mice: SKF38393; 6066.44 ± 409.09, SKF38393 + SL651498; 3359.67 ± 418.92 (P = 0.0053): Lenti-CAG-Comt-infected *Df1/+* mice: SKF38393; 4092.50 ± 516.66, SKF38393 + SL651498; 4391.67 ± 358.92 (P = 0.65): stereotypy count from 30 to 60 min after administration, Lenti-CAG-GFP-infected *Df1/+* mice: methamphetamine; 4104.63 ± 565.90, methamphetamine + bretazenil; 1984.60 ± 721.46 (P = 0.048), Lenti-CAG-Comt-infected *Df1/+* mice: methamphetamine; 3827.57 ± 1020.98, methamphetamine + bretazenil; 4696.33 ± 1240.41 (P = 0.60); Figures 6c, f and 7c). These results demonstrated that PFC *Comt* overexpression did not only suppress the high responsiveness of *Df1/+* mice to MK801 and SKF38393, but also attenuate the abnormal response to $GABA_A$ receptor agonists, suggesting that the curing effects of *Comt* overexpression might be through the regulation of GABAergic system.

Next, we examined whether the curing effects of *Comt* overexpression depend on Comt enzymatic activity. Tolcapone (30 mg kg^{-1}, i.p.) again failed to reverse the effects of bretazenil (stereotypy count from 30 to 60 min after administration, Lenti-CAG-Comt-infected *Df1/+* mice: methamphetamine + bretazenil; 4696.33 ± 1240.41, methamphetamine + bretazenil + tolcapone; 3141.67 ± 1379.29, (P = 0.42); Figure 7c). These data suggest that the curing effect on the responsiveness to $GABA_A$ receptor agonists might also be a secondary effect of increasing Comt activity.

***Comt* overexpression enhanced the responsiveness to $GABA_A$ receptor agonists in control mice.** We next examined the effects of PFC *Comt* overexpression on the behavioral responsiveness to $GABA_A$ receptor agonists in control mice. Lenti-CAG-Comt-infected mice showed enhanced responsiveness to a low dose of either bretazenil (10 mg kg^{-1}, i.p.) or SL651498 (1 mg kg^{-1}, i.p.) when treated with methamphetamine (1 mg kg^{-1}, i.p.) (stereotypy count, Lenti-CAG-Comt: methamphetamine; 4097.44 ± 537.31, methamphetamine + bretazenil; 1749.00 ± 640.53 (P = 0.017), methamphetamine + SL651498; 1664.71 ± 895.29 (P = 0.031); Figure 6a), whereas in Lenti-CAG-GFP-infected control mice, this dose of SL651498 had no effect on the locomotor stimulating effects of methamphetamine (stereotypy count, Lenti-CAG-GFP: methamphetamine; 3113.67 ± 577.52, methamphetamine + bretazenil; 3547.50 ± 875.70, P = 0.73, methamphetamine + SL651498; 3083.00 ± 1115.41, P = 0.98; Figure 7a). In addition, this effect of PFC *Comt* overexpression was also observed in mice infected by Lenti-CaMKII-Comt (stereotypy count, Lenti-CaMKII-Comt: methamphetamine; 3529.73 ± 679.80, methamphetamine +

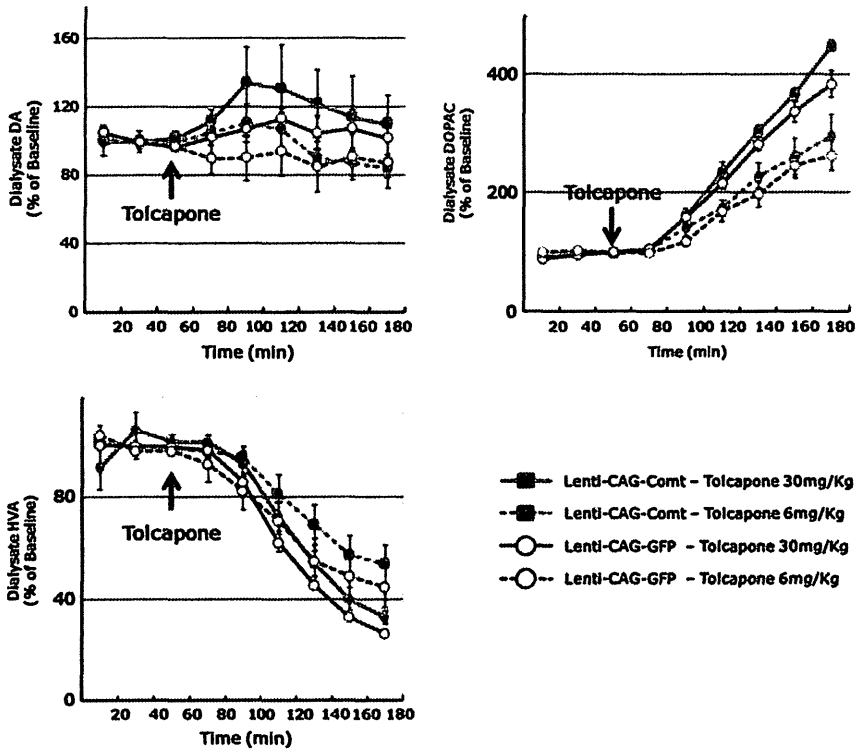

Figure 5 Effects of tolcapone on prefrontal cortex (PFC) extracellular dopamine (DA), 3,4-dihydroxyphenylacetic acid (DOPAC) and homovanillic acid (HVA) in Lenti-CAG-Comt or control Lenti-CAG-GFP mice. Three 20 min baseline fractions were collected before tolcapone (6 and 30 mg kg^{-1} intraperitoneally (i.p.)) injection and thereafter 20 min fractions were collected for 120 min. Data are means ± s.e.m. from three mice.

bretazenil; 1310.09 ± 400.01, $P=0.011$, methamphetamine + SL651498; 1546.80 ± 373.56, $P=0.022$; Figure 7a). These data suggest that the differences in *Comt* expression level in interneurons and astrocytes did not influence the effects of *Comt*-expressing lentiviruses on the responsiveness to $GABA_A$ receptor agonists. This high responsiveness of Lenti-CAG-Comt or Lenti-CaMKII-Comt-infected mice to bretazenil is also resistant to tolcapone (stereotypy count, Lenti-CAG-Comt: methamphetamine + bretazenil; 1749.000 ± 640.53, methamphetamine + bretazenil + tolcapone; 1628.08 ± 444.13, $P=0.88$, Lenti-CaMKII-Comt: methamphetamine + bretazenil; 1310.09 ± 400.01, methamphetamine + bretazenil + tolcapone; 1743.36 ± 524.16, $P=0.52$; Figure 7b), suggesting that the increasing Comt activity might indirectly cause an abnormal responsiveness to $GABA_A$ receptor agonists in control mice.

***Comt* inhibition enhanced the responsiveness to $GABA_A$ receptor agonists in wild-type mice.** Furthermore, we found that inhibition of endogenous Comt activity by tolcapone enhanced the responsiveness to bretazenil in methamphetamine-induced hyperlocomotion of Lenti-CAG-GFP-infected wild-type mice (Lenti-CAG-GFP: methamphetamine + bretazenil; 3547.50 ± 875.70, methamphetamine + bretazenil + tolcapone; 1523.30 ± 355.24, $P=0.046$; Figure 7b), whereas administration of tolcapone had no effects on locomotor effects of methamphetamine in Lenti-CAG-Comt, Lenti-CaMKII-Comt or Lenti-CAG-GFP-infected mice (Figure 7b). These data demonstrated that both elevation and reduction in Comt expression lead to an abnormal responsiveness to $GABA_A$ receptor agonists.

***Comt* overexpression induced c-Fos expression specifically in GABAergic interneurons.** It has been reported that NMDA antagonists increase PFC activity[37] and increase the expression of *c-Fos* specifically in pyramidal neurons but not in GABAergic interneurons.[38] To examine how increasing *Comt* expression affects PFC activity, we performed immunohistochemical analysis of c-Fos expression in the PFC of Lenti-CAG-Comt-, Lenti-CamKII-Comt- or Lenti-CAG-GFP-infected *Df1/+* and control mice. In the PFC of Lenti-CAG-Comt- or Lenti-CamKII-Comt-infected control mice, *Comt* overexpression increased the number of c-Fos^+ cells induced by MK801 (0.32 mg kg^{-1}, i.p.; +/+ mice: Lenti-CAG-Comt; 7.49 ± 0.45 × 10^{-4} cells μm^{-2} ($P=0.034$), Lenti-CaMKII-Comt; 7.74 ± 0.56 × 10^{-4} cells μm^{-2} ($P=0.021$), Lenti-CAG-GFP; 5.98 ± 0.21 × 10^{-4} cells μm^{-2}; Figures 8a and b). In contrast, in *Df1/+* mice, PFC *Comt* overexpression did not change the density of MK801-induced c-Fos^+ cells (*Df1/+* mice: Lenti-CAG-Comt; 2.09 ± 0.42 × 10^{-4} cells μm^{-2}, Lenti-CAG-GFP; 2.63 ± 0.18 × 10^{-4} cells μm^{-2}, $P=0.36$; Figures 8a and b). Double immunofluorescent studies of c-Fos and GABA revealed that the enhanced c-Fos expression was observed in GABAergic interneurons but not in GABA-negative cells in both superficial (II/III) and deep layers (V/VI) of Lenti-CAG-Comt-, Lenti-CamKII-Comt- and Lenti-CAG-GFP-infected control mice (+/+ mice: layer II/III,

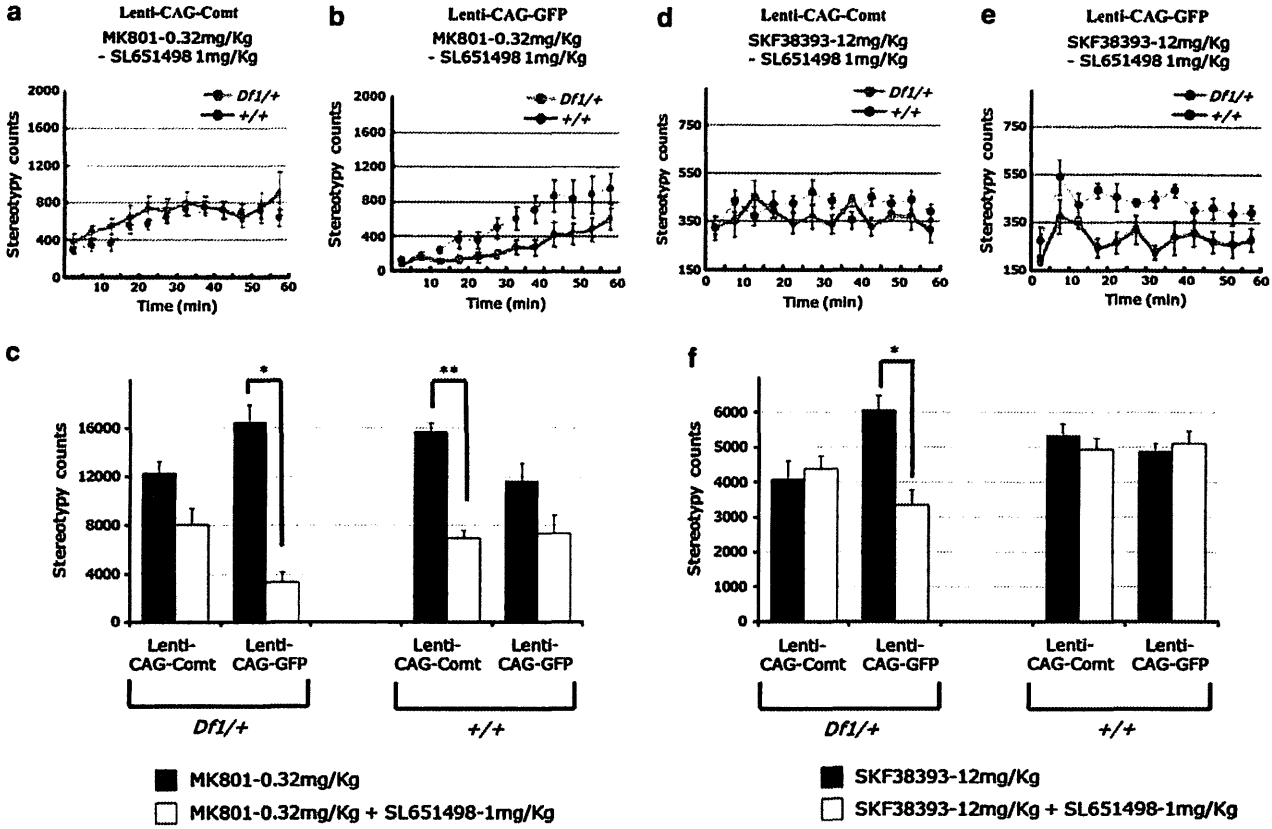

Figure 6 Normalization of the abnormal response of *Df1/+* mice to SL651498 by lentivirus-mediated *catechol-O-methytransferase* (*Comt*) overexpression in the prefrontal cortex (PFC). (**a–c**) MK801 (0.32 mg kg^{-1}) and (**d–f**) SL651498 (1 mg kg^{-1}), $GABA_A$ α2/α3 receptor agonist, were injected intraperitoneally and SKF38393 (12 mg kg^{-1}) was injected subcutaneously to the Lenti-CAG-Comt (**a, d**) or control Lenti-CAG-GFP (**b, e**)-infected *Df1/+* and control mice. Stereotypy count is shown in 5 min bins for 60 min after drug administration (**a, b, d, e**) and quantification of stereotypy count for 60 min is shown in (**c, f**). Values are the mean ± s.e.m. for 8–9 male mice. (**c**) $^*P = 0.0000022$, $^{**}P = 0.00000076$. (**f**) $^*P = 0.0053$.

c-Fos$^+$GABA$^+$ cells: Lenti-CAG-Comt; $4.2 \pm 0.47 \times 10^{-5}$ cells μm^{-2} ($P = 0.00045$), Lenti-CaMKII-Comt; $2.8 \pm 0.54 \times 10^{-4}$ cells μm^{-2} ($P = 0.0083$), Lenti-CAG-GFP; $4.7 \pm 2.7 \times 10^{-6}$ cells μm^{-2}, layer V/VI, c-Fos$^+$GABA$^+$ cells: Lenti-CAG-Comt; $2.3 \pm 0.27 \times 10^{-5}$ cells μm^{-2} ($P = 0.0038$), Lenti-CaMKII-Comt; $1.6 \pm 0.31 \times 10^{-4}$ cells μm^{-2} ($P = 0.074$), Lenti-CAG-GFP; $7.0 \pm 2.3 \times 10^{-6}$ cells μm^{-2}; Figures 8c and d). In *Df1/+* mice, PFC *Comt* overexpression also increased c-Fos expression in GABAergic interneurons (*Df1/+* mice: layer II/III, c-Fos$^+$GABA$^+$ cells: Lenti-CAG-Comt; $2.2 \pm 0.31 \times 10^{-5}$ cells μm^{-2}, Lenti-CAG-GFP; $6.2 \pm 3.1 \times 10^{-6}$ cells μm^{-2} ($P = 0.024$), layer V/VI, c-Fos$^+$ GABA$^+$ cells: Lenti-CAG-Comt; $2.5 \pm 0.31 \times 10^{-5}$ cells μm^{-2} ($P = 0.0078$), Lenti-CAG-GFP; $3.1 \pm 3.1 \times 10^{-6}$ cells μm^{-2}; Figures 8c and d). These data indicate that increasing *Comt* expression in the PFC specifically enhance the activity of interneurons in both *Df1/+* and control mice.

***Comt* overexpression upregulated GABA signaling-related genes in the PFC.** To examine the effects of *Comt* overexpression on GABA signaling, we assessed the expression levels of GABA receptors and GABA signaling-related genes at 2 weeks after infection by real-time PCR. We observed significant correlation between *Comt* expression and *Gabrb2* (*$GABA_A$receptor* β*2*), *Gad2* (*glutamic acid decarboxylase 65* (*GAD65*)) and *Reln* (*reelin*) in the PFC of Lenti-CAG-Comt-infected mice (*Gabrb2*: $R = 0.63$, $P = 0.020$, *Gad2*: $R = 0.63$, $P = 0.020$, and *Reln*: $R = 0.62$, $P = 0.023$; Figures 9a–c). Similar effects were also observed in Lenti-CaMKII-Comt-infected mice (*Gabrb2*: $R = 0.85$, $P = 0.0082$, *Gad2*: $R = 0.91$, $P = 0.0016$, and *Reln*: $R = 0.66$, $P = 0.077$; Figures 9a–c).

Next, we examined the effects of increasing *Comt* expression on GABAergic synapses in the PFC. GABA immunofluorescence in the prelimbic cortex was present as puncta rings around soma. Quantitative analysis of fluorescent pixel density of puncta rings showed that GABA immunofluorescence in perisomatic puncta was increased by Lenti-CAG-Comt or Lenti-CaMKII-Comt infection in both *Df1/+* and control mice (pixel density, +/+ mice: Lenti-CAG-Comt; 1552.06 ± 93.11 ($P = 0.026$), Lenti-CaMKII-Comt; 1638.72 ± 67.61 ($P = 0.0067$), Lenti-CAG-GFP; 1169.67 ± 60.57; Figures 3d, e, g and h). However, there was no change in the density of Gad67$^+$ cells (+/+ mice, Lenti-CAG-Comt; $1.61 \pm 0.097 \times 10^{-4}$ cells μm^{-2} ($P = 0.81$), Lenti-CaMKII-Comt; $1.86 \pm 0.22 \times 10^{-4}$ cells μm^{-2} ($P = 0.29$), Lenti-CAG-GFP; $1.55 \pm 0.16 \times 10^{-4}$ cells μm^{-2}). These data showed that *Comt* overexpression enhanced GABA production without affecting the number of GABAergic interneurons and that the differences in the *Comt* expression levels in interneurons

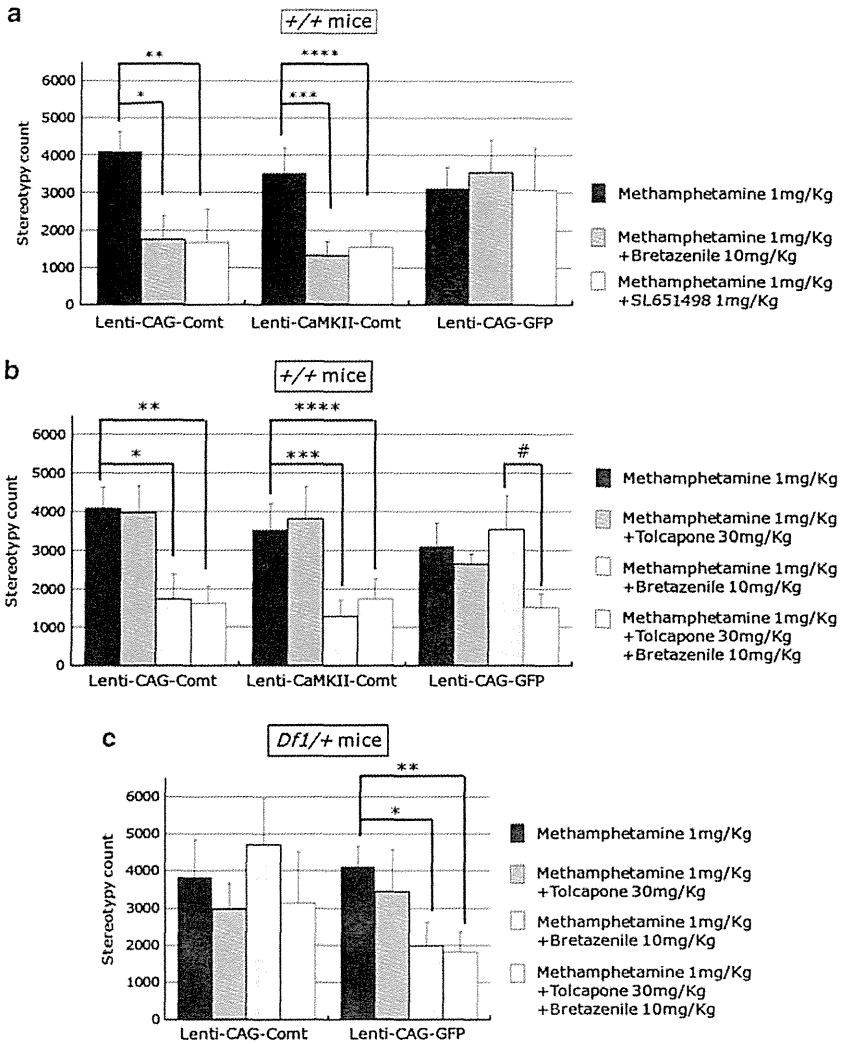

Figure 7 The enzymatic activity-independent or activity-dependent effects of *catechol-O-methytransferase* (*Comt*) on the responsiveness to $GABA_A$ receptor agonists. (**a**) Prefrontal cortex (PFC) *Comt* overexpression in the Lenti-CAG-Comt- or Lenti-CaMKII-Comt-infected control mice enhanced the response to bretazenil, a $GABA_A$ receptor agonist, and SL651498. Methamphetamine (1 mg kg^{-1}) was intraperitoneally injected with bretazenil (10 mg kg^{-1}) or SL651498 (1 mg kg^{-1}). Stereotypy count from 30 to 60 min after methamphetamine administration is shown. Values are the mean ± s.e.m. for 6–10 male mice. $^{*}P=0.017$, $^{**}P=0.031$, $^{***}P=0.011$, $^{****}P=0.022$. (**b**) Tolcapone failed to reverse the enhanced responsiveness to bretazenil in PFC COMT-overexpressing mice, but increased the responsiveness to bretazenil in GFP-expressing control mice. Tolcapone (30 mg kg^{-1}) was intraperitoneally injected to Lenti-CAG-Comt or -GFP-infected control mice 1 h before administration of methamphetamine (1 mg kg^{-1}). Stereotypy count from 30 to 60 min after methamphetamine administration is shown. Values are the mean ± s.e.m. for 6–13 male mice. $^{*}P=0.017$, $^{**}P=0.031$, $^{***}P=0.011$, $^{****}P=0.050$, $^{\#}P=0.026$. (**c**) Tolcapone failed to reverse the treatment effect of *Comt* overexpression on the enhanced responsiveness to bretazenil in *Df1/+* mice. Tolcapone (30 mg kg^{-1}) was intraperitoneally injected to Lenti-CAG-Comt or -GFP-infected *Df1/+* or control mice 1 h before administration of methamphetamine (1 mg kg^{-1}). Stereotypy count from 30 to 60 min after methamphetamine administration is shown. Values are the mean ± s.e.m. for 6–13 male mice. $^{*}P=0.048$, $^{**}P=0.019$.

and astrocytes did not change the enhancing effects on GABA transmission.

Finally, we examined the effects of *Comt* overexpression on GABA release in the PFC by *in vivo* microdialysis. In control mice, PFC *Comt* overexpression drastically increased GABA release after MK801 administration (0.32 mg kg^{-1}, i.p.; virus-by-time interaction on GABA level: $F_{8,32}=5.60$, $n=3$ per group, $P=0.0062$ (repeated two-way ANOVA); Figure 10), although no statistically significant increase in GABA release was observed in *Comt*-overexpressing *Df1/+* mice (virus-by-time interaction on GABA level: $F_{8,40}=1.34$, $n=3$–4 per group, $P=0.25$ (repeated two-way ANOVA); Figure 10).

Discussion

Df1/+ mice displayed higher locomotive activity to psychostimulants, similar to human schizophrenic patients. Our pharmacological data suggest that GABA signaling abnormalities are involved in these behavioral abnormalities of *Df1/+* mice. Lentivirus-mediated *Comt* reintroduction to the PFC of *Df1/+* mice normalized the abnormal responses of *Df1/+* mice to $GABA_A$ receptor agonists as well as to psychostimulants. In contrast, in wild-type mice, increased *Comt* expression in the PFC caused abnormal responses to $GABA_A$ receptor agonists. A Comt inhibitor, tolcapone, failed

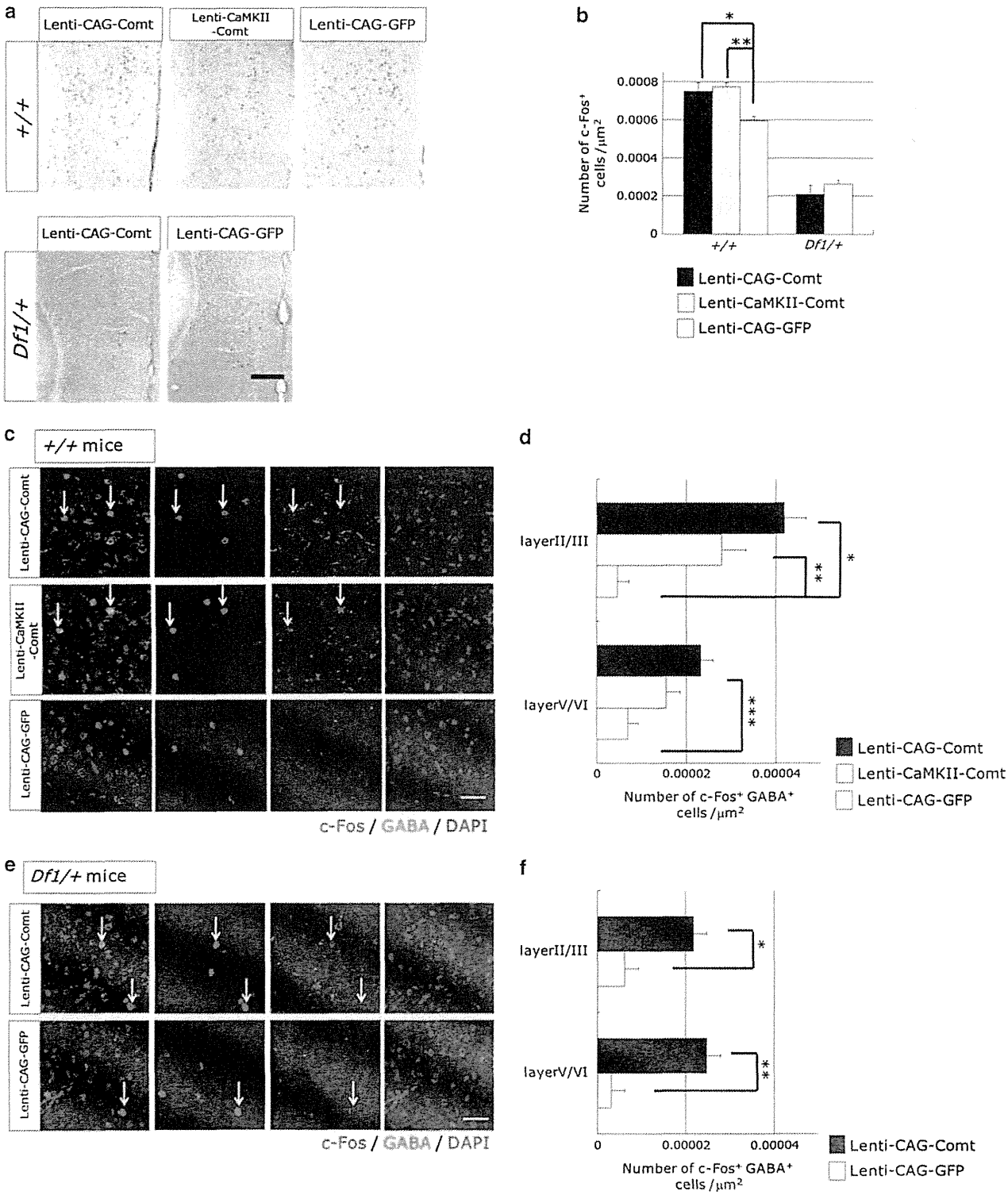

Figure 8 The effects of increasing *catechol-O-methytransferase* (*Comt*) expression on MK801-induced-c-Fos expression in the prefrontal cortex (PFC). (**a**, **b**) PFC *Comt* overexpression increased the number of MK801-induced-c-Fos-positive cells in control mice but not in *Df1/+* mice. Lenti-CAG-Comt-, Lenti-CaMKII-Comt- or Lenti-CAG-GFP-infected *Df1/+* or control mice were killed 2 h after MK801 (0.32 mg kg^{-1}) administration. Representative images of immunohistochemical studies for c-Fos from coronal sections of the prelimbic cortex (PrL; anterior/posterior = + 1.9 mm) are shown. Scale bar = 200 μm. Quantification of the density of c-Fos immunoreactive cells was performed (**b**). Values are the mean ± s.e.m. for 4–6 mice. $^{*}P = 0.034$, $^{**}P = 0.021$. (**c**, **d**) *Comt* overexpression increased c-Fos expression specifically in γ-aminobutyric acid (GABA)-positive cells in both control and *Df1/+* mice. Representative images of immunofluorescent studies for c-Fos (green), GABA (red) and 4′,6-diamidino-2-phenylindole (DAPI) staining of nuclei (blue) (**c**, **e**). Scale bar = 20 μm. The density of c-Fos^{+} $GABA^{+}$ cells (arrows) was measured in the layer II/III and the layer IV/V of the prelimbic cortex of Lenti-CAG-Comt-, Lenti-CaMKII-Comt- or Lenti-CAG-GFP-infected control (**d**) and *Df1/+* mice (**f**). Values are the mean ± s.e.m. of 4–6 mice (**d**) and 3 mice (**f**). (**d**) $^{*}P = 0.00045$, $^{**}P = 0.0083$, $^{***}P = 0.0038$, (**f**) $^{*}P = 0.024$, $^{**}P = 0.0078$.

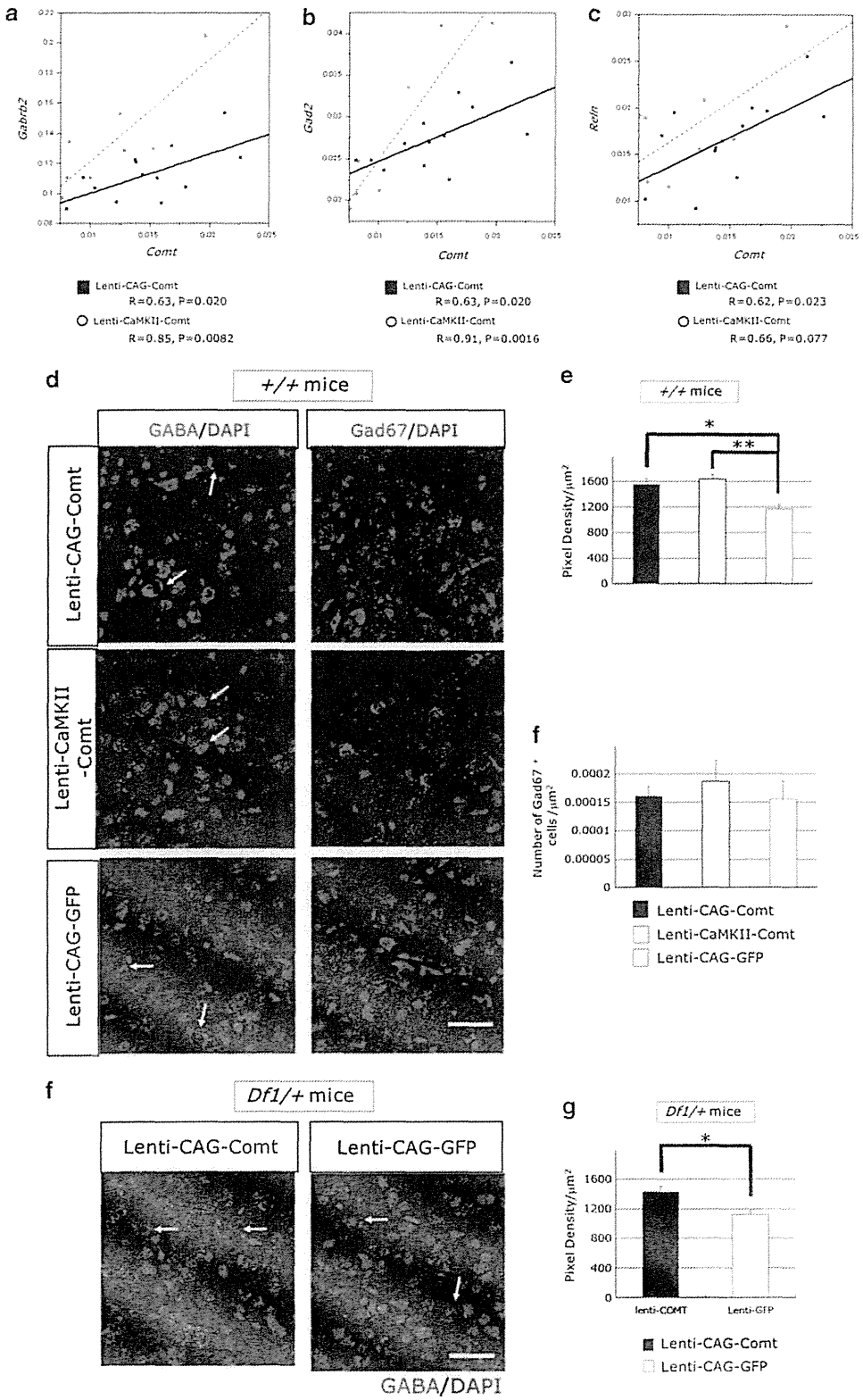

Figure 9 The effects of increasing *catechol-O-methytransferase* (*Comt*) expression on γ-aminobutyric acid (GABA)-related molecules in the prefrontal cortex (PFC). (**a**–**c**) The expression level of *Comt* correlates with GABA signaling-related genes, *Gabrb2* (*$GABA_A$receptor β2*) (**a**), *Gad2* (*Gad67*) (**b**) and *Reln* (*reelin*) (**c**). *Comt*, *Gabrb2*, *Gad2* and *Reln* were quantified and normalized to *Gapdh* of the PFC of Lenti-CAG-Comt- or Lenti-CaMKII-Comt-infected mice using real-time PCR. Mice were killed 2 weeks after lentiviral infection. A solid line depicts the linear regression for Lenti-CAG-Comt-infected mice, and a dashed line is for Lenti-CaMKII-Comt-infected mice. (**d**–**h**) Increased synaptic puncta of interneurons in the PFC of Lenti-CAG-Comt- or Lenti-CaMKII-Comt-infected control mice (**d**–**f**) and *Df1/+* mice (**g**, **h**). Fluorescent puncta rings surrounding unlabeled soma are shown by arrows (**d**, **g**). Quantification of immunofluorescent intensity of GABA in puncta rings (**e**, **h**) and the density of $Gad67^+$ cells (**f**). Scale = 20 μm. Values are the mean ± s.e.m. of 3–4 mice. (e) $^*P = 0.026$, $^{**}P = 0.0067$, (h) $^*P = 0.0037$.

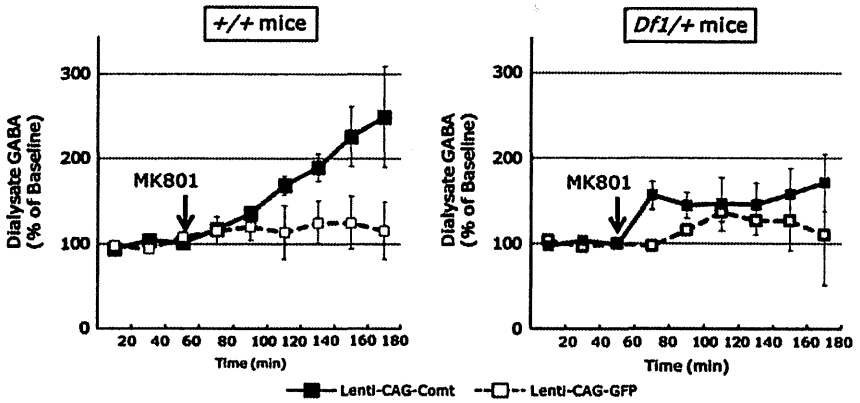

Figure 10 Effects of MK801 on prefrontal cortex (PFC) extracellular γ-aminobutyric acid (GABA) in Lenti-CAG-Comt or control Lenti-CAG-GFP-infected *Df1/+* and control mice. Three 20 min baseline fractions were collected before MK801 (0.32 mg kg^{-1}, intraperitoneally (i.p.)) injection and thereafter 20 min fractions were collected for 120 min. Data are means ± s.e.m. from 3 to 4 mice.

to reverse the curing effect of *Comt* overexpression on behavioral abnormalities of *Df1/+* mice, indicating that the effects do not directly result from increased Comt enzymatic activity in the PFC. *Comt* overexpression in the PFC upregulated GABA signaling-related genes, which might explain the effects of Comt overexpression on GABA signaling. Furthermore, we showed PFC *Comt* expression increased c-Fos expression specifically in GABAergic interneurons and enhanced MK801-induced GABA release.

Deficits in the GABAergic system are thought to be one of the prominent pathologies of schizophrenia.[32–34] Postmortem studies of the brains of schizophrenic patients showed reduction in the 67 kDa isoform of GAD (GAD67), which is an enzyme responsible for GABA synthesis.[39,40] GAD67 reduction is observed specifically in chandelier cells.[41] Decrease in GABA reuptake transporter and upregulation of $GABA_A$ α2 receptor are also observed at chandelier cell synapse of schizophrenic patients, which might compensate the reduction of GABAergic transmission caused by GAD67 reduction.[42–44] The abnormal development of parvalbumin-positive interneurons including chandelier cells has been shown in a different mouse model of 22q11DS.[45] Our data showed the abnormal responsiveness of *Df1/+* mice to a $GABA_A$ receptor agonist (bretazenil) and a $GABA_A$ receptor α2/α3 agonist (SL651498) in psychostimulant-induced hyperlocomotion. *Comt* overexpression in the PFC not only normalized abnormal responsiveness of *Df1/+* mice to psychostimulants, but also attenuated the abnormal responsiveness to $GABA_A$ receptor agonist. Our studies also demonstrated that increasing *Comt* activity in the PFC caused upregulation of GABA-related genes such as *Gabrb2*, *Gad2* and *Reln*. Single-nucleotide polymorphisms of *RELN* and *GABRB2* are known to associated with risks for schizophrenia.[46,47] *Reln* is reported to be expressed in GABAergic neurons, and affects the composition of NMDA receptors.[48] NMDA receptors regulate the activity of fast-spiking interneurons, and NMDA antagonists decrease the activity of interneurons in the PFC, leading to excitation of cortical pyramidal neurons by disinhibition.[49] Increase in GABA level at the interneuronal synapses and GABA release was observed in PFC *Comt*-overexpressing mice, which might be caused by increased level of *Gad2*. This enhanced GABA transmission might be responsible for the treatment effects of *Comt* overexpression. Our finding of the regulation of GABA signaling by Comt is consistent with a previous report that shows the genetic association of *COMT* with cortical GABA level.[50]

DA is known to modulate GABA transmission in multiple brain regions. Electrically evoked GABA release was reduced by D2 agonists in the PFC and the striatum,[51,52] but spontaneous release of GABA was increased by D2 agonists in the PFC.[52] Electrophysiological studies have shown that DA produces an initial reduction in inhibitory postsynaptic current in PFC pyramidal neurons through the reduction in GABA release, probability mediated by D2 receptor, followed by a long-lasting increase in inhibitory postsynaptic current amplitude, which is mainly mediated by D1 receptor.[53] Different effects of DA on GABA transmission have been reported, and the molecular mechanism of the effects of *Comt* overexpression on GABA transmission remains to be elucidated.

A *COMT* low-activity allele is identified as a risk factor for impaired cognitive function and psychiatric symptoms in adolescence in 22q11DS.[14–17] Epistatic interaction between *Comt* and *Prodh* is known to modulate schizophrenia-like phenotypes in mice.[7] Our data are consistent with these findings. Our studies demonstrate that *Comt* overexpression in the PFC has a curing effect on *Df1/+* mice and that *Comt* has dual roles in the regulation of responsiveness to $GABA_A$ receptor agonists. The high Comt activity enhanced the GABA production and GABA release in the PFC and increased the responsiveness to $GABA_A$ receptor agonists, whereas endogenous relatively low Comt activity seemed to have the opposite effects, because a Comt inhibitor increased the responsiveness to $GABA_A$ receptor agonist in methamphetamine-induced locomotion of control mice. This phenotype of tolcapone-treated mice is similar to *Df1/+* mice, which have Comt heterozygosity. It is tempting to speculate the existence of inverted U-shaped relationship between Comt-regulated cortical DA level and GABA transmissional regulation.

Our pharmacological data suggest that $GABA_A$ α2/α3 receptor might be a therapeutic target for psychiatric

symptoms of 22q11DS, although conflicting results were obtained for therapeutic effects of $GABA_A$ α2/α3 receptor agonist for general schizophrenia.[54,55] Schizophrenia is considered to be a heterogeneous group of disorders, and individual tailor-made drug treatment might be required for effective treatment of schizophrenia patients according to the disease etiology. In addition, pharmacological treatments to increase *Comt* expression or activity also can be used to reduce or prevent psychiatric symptoms of 22q11DS. However, therapeutic intervention should take into account the dual roles of Comt in the regulation of GABA transmission.

Conflict of interest

The authors declare no conflict of interest.

Acknowledgements. We thank Carlos Lois and Pavel Osten for FUGW and Δ8.9 and VSVG plasmids. This work was supported by NOVARTIS Foundation for the Promotion of Science and Uehara Memorial Foundation.

1. Pulver AE, Nestadt G, Goldberg R, Shprintzen RJ, Lamacz M, Wolyniec PS *et al.* Psychotic illness in patients diagnosed with velo-cardio-facial syndrome and their relatives. *J Nerv Ment Dis* 1994; **182**: 476–478.
2. Karayiorgou M, Morris MA, Morrow B, Shprintzen RJ, Goldberg R, Borrow J *et al.* Schizophrenia susceptibility associated with interstitial deletions of chromosome 22q11. *Proc Natl Acad Sci USA* 1995; **92**: 7612–7616.
3. Manolio TA, Collins FS, Cox NJ, Goldstein DB, Hindorff LA, Hunter DJ *et al.* Finding the missing heritability of complex diseases. *Nature* 2009; **461**: 747–753.
4. Puech A, Saint-Jore B, Funke B, Gilbert DJ, Sirotkin H, Copeland NG *et al.* Comparative mapping of the human 22q11 chromosomal region and the orthologous region in mice reveals complex changes in gene organization. *Proc Natl Acad Sci USA* 1997; **94**: 14608–14613.
5. Paylor R, McIlwain KL, McAninch R, Nellis A, Yuva-Paylor LA, Baldini A *et al.* Mice deleted for the DiGeorge/velocardiofacial syndrome region show abnormal sensorimotor gating and learning and memory impairments. *Hum Mol Genet* 2001; **10**: 2645–2650.
6. Stark KL, Xu B, Bagchi A, Lai WS, Liu H, Hsu R *et al.* Altered brain microRNA biogenesis contributes to phenotypic deficits in a 22q11-deletion mouse model. *Nat Genet* 2008; **40**: 751–760.
7. Paterlini M, Zakharenko SS, Lai WS, Qin J, Zhang H, Mukai J *et al.* Transcriptional and behavioral interaction between 22q11.2 orthologs modulates schizophrenia-related phenotypes in mice. *Nat Neurosci* 2005; **8**: 1586–1594.
8. Scatton B, Dubois A, Dubocovich ML, Zahniser NR, Fage D. Quantitative autoradiography of 3H-nomifensine binding sites in rat brain. *Life Sci* 1985; **36**: 815–822.
9. Sesack SR, Hawrylak VA, Matus C, Guido MA, Levey AI. Dopamine axon varicosities in the prelimbic division of the rat prefrontal cortex exhibit sparse immunoreactivity for the dopamine transporter. *J Neurosci* 1998; **18**: 2697–2708.
10. Gogos JA, Morgan M, Luine V, Santha M, Ogawa S, Pfaff D *et al.* Catechol-O-methyltransferase-deficient mice exhibit sexually dimorphic changes in catecholamine levels and behavior. *Proc Natl Acad Sci USA* 1998; **95**: 9991–9996.
11. Moron JA, Brockington A, Wise RA, Rocha BA, Hope BT. Dopamine uptake through the norepinephrine transporter in brain regions with low levels of the dopamine transporter: evidence from knock-out mouse lines. *J Neurosci* 2002; **22**: 389–395.
12. Miner LH, Schroeter S, Blakely RD, Sesack SR. Ultrastructural localization of the norepinephrine transporter in superficial and deep layers of the rat prelimbic prefrontal cortex and its spatial relationship to probable dopamine terminals. *J Comp Neurol* 2003; **466**: 478–494.
13. Tunbridge E, Burnet PW, Sodhi MS, Harrison PJ. Catechol-o-methyltransferase (COMT) and proline dehydrogenase (PRODH) mRNAs in the dorsolateral prefrontal cortex in schizophrenia, bipolar disorder, and major depression. *Synapse* 2004; **51**: 112–118.
14. Gothelf D, Eliez S, Thompson T, Hinard C, Penniman L, Feinstein C *et al.* COMT genotype predicts longitudinal cognitive decline and psychosis in 22q11.2 deletion syndrome. *Nat Neurosci* 2005; **8**: 1500–1502.
15. Baker K, Baldeweg T, Sivagnanasundaram S, Scambler P, Skuse D. COMT Val108/158 Met modifies mismatch negativity and cognitive function in 22q11 deletion syndrome. *Biol Psychiatry* 2005; **58**: 23–31.
16. Lachman HM, Morrow B, Shprintzen R, Veit S, Parsia SS, Faedda G *et al.* Association of codon 108/158 catechol-O-methyltransferase gene polymorphism with the psychiatric manifestations of velo-cardio-facial syndrome. *Am J Med Genet* 1996; **67**: 468–472.
17. Michaelovsky E, Gothelf D, Korostishevsky M, Frisch A, Burg M, Carmel M *et al.* Association between a common haplotype in the COMT gene region and psychiatric disorders in individuals with 22q11.2DS. *Int J Neuropsychopharmacol* 2008; **11**: 351–363.
18. Kates WR, Antshel KM, Abdulsabur N, Colgan D, Funke B, Fremont W *et al.* A gender-moderated effect of a functional COMT polymorphism on prefrontal brain morphology and function in velo-cardio-facial syndrome (22q11.2 deletion syndrome). *Am J Med Genet B Neuropsychiatr Genet* 2006; **141B**: 274–280.
19. Bearden CE, Jawad AF, Lynch DR, Sokol S, Kanes SJ, McDonald-McGinn DM *et al.* Effects of a functional COMT polymorphism on prefrontal cognitive function in patients with 22q11.2 deletion syndrome. *Am J Psychiatry* 2004; **161**: 1700–1702.
20. Shashi V, Keshavan MS, Howard TD, Berry MN, Basehore MJ, Lewandowski E *et al.* Cognitive correlates of a functional COMT polymorphism in children with 22q11.2 deletion syndrome. *Clin Genet* 2006; **69**: 234–238.
21. Williams GV, Goldman-Rakic PS. Modulation of memory fields by dopamine D1 receptors in prefrontal cortex. *Nature* 1995; **376**: 572–575.
22. Mattay VS, Goldberg TE, Fera F, Hariri AR, Tessitore A, Egan MF *et al.* Catechol O-methyltransferase val158-met genotype and individual variation in the brain response to amphetamine. *Proc Natl Acad Sci USA* 2003; **100**: 6186–6191.
23. Papaleo F, Crawley JN, Song J, Lipska BK, Pickel J, Weinberger DR *et al.* Genetic dissection of the role of catechol-O-methyltransferase in cognition and stress reactivity in mice. *J Neurosci* 2008; **28**: 8709–8723.
24. Maynard TM, Haskell GT, Peters AZ, Sikich L, Lieberman JA, LaMantia AS. A comprehensive analysis of 22q11 gene expression in the developing and adult brain. *Proc Natl Acad Sci USA* 2003; **100**: 14433–14438.
25. Stanwood GD, Parlaman JP, Levitt P. Anatomical abnormalities in dopaminoceptive regions of the cerebral cortex of dopamine D1 receptor mutant mice. *J Comp Neurol* 2005; **487**: 270–282.
26. Kim SY, Choi KC, Chang MS, Kim MH, Kim SY, Na YS *et al.* The dopamine D2 receptor regulates the development of dopaminergic neurons via extracellular signal-regulated kinase and Nurr1 activation. *J Neurosci* 2006; **26**: 4567–4576.
27. Earls LR, Bayazitov IT, Fricke RG, Berry RB, Illingworth E, Mittleman G *et al.* Dysregulation of presynaptic calcium and synaptic plasticity in a mouse model of 22q11 deletion syndrome. *J Neurosci* 2011; **30**: 15843–15855.
28. Lois C, Hong EJ, Pease S, Brown EJ, Baltimore D. Germline transmission and tissue-specific expression of transgenes delivered by lentiviral vectors. *Science* 2002; **295**: 868–872.
29. Lahti AC, Koffel B, LaPorte D, Tamminga CA. Subanesthetic doses of ketamine stimulate psychosis in schizophrenia. *Neuropsychopharmacology* 1995; **13**: 9–19.
30. Malhotra AK, Pinals DA, Adler CM, Elman I, Clifton A, Pickar D *et al.* Ketamine-induced exacerbation of psychotic symptoms and cognitive impairment in neuroleptic-free schizophrenics. *Neuropsychopharmacology* 1997; **17**: 141–150.
31. Szeszko PR, Bilder RM, Dunlop JA, Walder DJ, Lieberman JA. Longitudinal assessment of methylphenidate effects on oral word production and symptoms in first-episode schizophrenia at acute and stabilized phases. *Biol Psychiatry* 1999; **45**: 680–686.
32. Perry TL, Kish SJ, Buchanan J, Hansen S. Gamma-aminobutyric-acid deficiency in brain of schizophrenic patients. *Lancet* 1979; **1**: 237–239.
33. Benes FM, Berretta S. GABAergic interneurons: implications for understanding schizophrenia and bipolar disorder. *Neuropsychopharmacology* 2001; **25**: 1–27.
34. Lewis DA, Hashimoto T, Volk DW. Cortical inhibitory neurons and schizophrenia. *Nat Rev Neurosci* 2005; **6**: 312–324.
35. Xu B, Roos JL, Dexheimer P, Boone B, Plummer B, Levy S *et al.* Exome sequencing supports a de novo mutational paradigm for schizophrenia. *Nat Genet* 2011; **43**: 864–868.
36. Niwa H, Yamamura K, Miyazaki J. Efficient selection for high-expression transfectants with a novel eukaryotic vector. *Gene* 1991; **108**: 193–199.
37. Breier A, Malhotra AK, Pinals DA, Weisenfeld NI, Pickar D. Association of ketamine-induced psychosis with focal activation of the prefrontal cortex in healthy volunteers. *Am J Psychiatry* 1997; **154**: 805–811.
38. Kargieman L, Santana N, Mengod G, Celada P, Artigas F. Antipsychotic drugs reverse the disruption in prefrontal cortex function produced by NMDA receptor blockade with phencyclidine. *Proc Natl Acad Sci USA* 2007; **104**: 14843–14848.
39. Akbarian S, Kim JJ, Potkin SG, Hagman JO, Tafazzoli A, Bunney Jr WE *et al.* Gene expression for glutamic acid decarboxylase is reduced without loss of neurons in prefrontal cortex of schizophrenics. *Arch Gen Psychiatry* 1995; **52**: 258–266.
40. Volk DW, Austin MC, Pierri JN, Sampson AR, Lewis DA. Decreased glutamic acid decarboxylase67 messenger RNA expression in a subset of prefrontal cortical gamma-aminobutyric acid neurons in subjects with schizophrenia. *Arch Gen Psychiatry* 2000; **57**: 237–245.
41. Lewis DA, Gonzalez-Burgos G. Pathophysiologically based treatment interventions in schizophrenia. *Nat Med* 2006; **12**: 1016–1022.
42. Woo TU, Whitehead RE, Melchitzky DS, Lewis DA. A subclass of prefrontal gamma-aminobutyric acid axon terminals are selectively altered in schizophrenia. *Proc Natl Acad Sci USA* 1998; **95**: 5341–5346.
43. Volk DW, Pierri JN, Fritschy JM, Auh S, Sampson AR, Lewis DA. Reciprocal alterations in pre- and postsynaptic inhibitory markers at chandelier cell inputs to pyramidal neurons in schizophrenia. *Cereb Cortex* 2002; **12**: 1063–1070.
44. Volk D, Austin M, Pierri J, Sampson A, Lewis D. GABA transporter-1 mRNA in the prefrontal cortex in schizophrenia: decreased expression in a subset of neurons. *Am J Psychiatry* 2001; **158**: 256–265.

45. Meechan DW, Tucker ES, Maynard TM, LaMantia AS. Diminished dosage of 22q11 genes disrupts neurogenesis and cortical development in a mouse model of 22q11 deletion/ DiGeorge syndrome. *Proc Natl Acad Sci USA* 2009; **106**: 16434–16445.
46. Shifman S, Johannesson M, Bronstein M, Chen SX, Collier DA, Craddock NJ *et al.* Genome-wide association identifies a common variant in the reelin gene that increases the risk of schizophrenia only in women. *PLoS Genet* 2008; **4**: e28.
47. Zhao C, Xu Z, Chen J, Yu Z, Tong KL, Lo WS *et al.* Two isoforms of GABA(A) receptor beta2 subunit with different electrophysiological properties: differential expression and genotypical correlations in schizophrenia. *Mol Psychiatry* 2006; **11**: 1092–1105.
48. Campo CG, Sinagra M, Verrier D, Manzoni OJ, Chavis P. Reelin secreted by GABAergic neurons regulates glutamate receptor homeostasis. *PLoS One* 2009; **4**: e5505.
49. Homayoun H, Moghaddam B. NMDA receptor hypofunction produces opposite effects on prefrontal cortex interneurons and pyramidal neurons. *J Neurosci* 2007; **27**: 11496–11500.
50. Marenco S, Savostyanova AA, van der Veen JW, Geramita M, Stein A, Barnett AS *et al.* Genetic modulation of GABA levels in the anterior cingulate cortex by GAD1 and COMT. *Neuropsychopharmacology* 2010; **35**: 1708–1717.
51. Harsing Jr LG, Zigmond MJ. Influence of dopamine on GABA release in striatum: evidence for D1-D2 interactions and non-synaptic influences. *Neuroscience* 1997; **77**: 419–429.
52. Retaux S, Besson MJ, Penit-Soria J. Opposing effects of dopamine D2 receptor stimulation on the spontaneous and the electrically evoked release of [3H]GABA on rat prefrontal cortex slices. *Neuroscience* 1991; **42**: 61–71.
53. Seamans JK, Gorelova N, Durstewitz D, Yang CR. Bidirectional dopamine modulation of GABAergic inhibition in prefrontal cortical pyramidal neurons. *J Neurosci* 2001; **21**: 3628–3638.
54. Lewis DA, Cho RY, Carter CS, Eklund K, Forster S, Kelly MA *et al.* Subunit-selective modulation of GABA type A receptor neurotransmission and cognition in schizophrenia. *Am J Psychiatry* 2008; **165**: 1585–1593.
55. Buchanan RW, Keefe RS, Lieberman JA, Barch DM, Csernansky JG, Goff DC *et al.* A randomized clinical trial of MK-0777 for the treatment of cognitive impairments in people with schizophrenia. *Biol Psychiatry* 2011; **69**: 442–449.

European Journal of Immunology

Notch signaling regulates the development of a novel type of Thy1-expressing dendritic cell in the thymus

Chieko Ishifune[1], Yoichi Maekawa[1], Jun Nishida[1], Akiko Kitamura[1], Kenji Tanigaki[2], Hideo Yagita[3] and Koji Yasutomo[1]

[1] Department of Immunology and Parasitology, Institute of Health Biosciences, The University of Tokushima Graduate School, Tokushima, Japan
[2] Shiga Research Center, Japan
[3] Department of Immunology, Juntendo University, Tokyo, Japan

Dendritic cells (DCs) are specialized antigen-presenting cells (APCs) required for T-cell activation and are classified into several subtypes by phenotypic and functional characteristics. However, it remains unclear if distinct transcription factors control the development of each DC subpopulation. In this report, we demonstrate that Notch signaling controls the development of a novel DC subtype that expresses Thy1 (Thy1$^+$DCs). Overstimulation of bone marrow cells with the Notch ligand Delta-like 1 promoted the development of Thy1$^+$DCs. Thy1$^+$DCs are characterized as CD11c$^+$MHC class II$^+$NK1.1$^-$B220$^-$CD8α^+, and are present in the thymus but not in the spleen and lymph nodes. Thymic Thy1$^+$DCs are able to capture exogenous proteins and delete CD4$^+$CD8$^+$ T cells. Transplantation experiments demonstrated that CD44$^+$CD25$^-$ and CD44$^+$CD25$^+$ thymocytes can differentiate into Thy1$^+$DCs. Recombination signal binding protein for immunoglobulin kappa J region (RBP-J) deficiency in lineage-negative bone marrow cells, but not CD11c$^+$ cells, disrupted Thy1$^+$DC development in the thymus. Our data indicate that Notch signaling controls the development of a novel type of Thy1-expressing DC in the thymus that possibly controls negative selection, and indicates that there may be highly regulated, differential transcriptional control of DC development. Furthermore, our findings suggest that Notch signaling regulates T-cell development not only by intrinsically inducing T-cell lineage-specific gene programs, but also by regulating negative selection through Thy1$^+$DCs.

Keywords: DCs · Differentiation · Notch

Supporting Information available online

Introduction

Dendritic cells (DCs) are specialized antigen-presenting cells (APCs) required for efficient T-cell activation and differentiation [1, 2]. DCs are characterized as possessing a dendritic morphology and the ability to present antigen efficiently, and they express CD11c and MHC class II (cII). DCs are classified into several subtypes based on phenotypic and functional characteristics. For instance, plasmacytoid DCs (pDCs) that express B220 and PDCA-1 are known to produce type I interferon after TLR9 stimulation [3]. The development of pDCs is controlled by the transcription factor E2-2, which does not affect the development of other DC subtypes [4]. Another study reported that PU.1 is crucial for both pDCs and conventional DCs [5]. Therefore, these data suggest that the development of each DC subtype is regulated by a subtype-specific transcription factor together with common sets of transcription factors.

Correspondence: Dr. Koji Yasutomo
e-mail: yasutomo@basic.med.tokushima-u.ac.jp

Notch signaling controls fate decision, survival and differentiation of cells [6]. The interaction of Notch and its ligands cleaves the transmembrane domain of Notch. Cleaved Notch translocates into the nucleus and interacts with recombination signal binding protein for immunoglobulin kappa J region (RBP-J), which is an essential transcription factor for Notch signaling. We and other groups have demonstrated that Notch controls lymphocyte development and functional differentiation [7–11]. Furthermore, several groups have demonstrated that Notch regulates DC differentiation. For instance, RBP-J deficiency in CD11c-positive cells disturbs the survival of $CD8^-$DCs, which decreases the number of $CD8^-$DCs [12]. This study also demonstrated that the number of pDCs is increased in RBP-J-deficient mice [12].